Plant and Cell Physiology Advance Access published June 21, 2016

PCP
PLANT & CELL PHYSIOLOGY

# HSI2 Repressor Recruits MED13 and HDA6 to Down-Regulate Seed Maturation Gene Expression Directly During Arabidopsis Early Seedling Growth

Tory Chhun[1], Suet Yen Chong[1], Bong Soo Park[1], Eriko Chi Cheng Wong[1], Jun-Lin Yin[1], Mijung Kim[1] Nam-Hai Chua[2,*]

[1]Temasek Life Sciences Laboratory, National University of Singapore, 1 Research Link, Singapore 117604, Singapore
[2]Laboratory of Plant Molecular Biology, The Rockefeller University, 1230 York Avenue, New York, NY 10065-6399, USA
*Corresponding author: Fax, +1-212-327-8327; E-mail, chua@rockefeller.edu
(Received March 7, 2016; Accepted May 1, 2016)

**Arabidopsis HSI2 (HIGH-LEVEL EXPRESSION OF SUGAR-INDUCIBLE GENE 2) which carries a EAR (ERF-associated amphiphilic repression) motif acts as a repressor of seed maturation genes and lipid biosynthesis, whereas MEDIATOR (MED) is a conserved multiprotein complex linking DNA-bound transcription factors to RNA polymerase II transcription machinery. How HSI2 executes its repressive function through MED is hitherto unknown. Here, we show that HSI2 and its homolog, HSI2-lik (HSL1), are able to form homo- and heterocomplexes. Both factors bind to the TRAP240 domain of MED13, a subunit of the MED CDK8 module. Mutant alleles of the *med13* mutant show elevated seed maturation gene expression and increased lipid accumulation in cotyledons; in contrast, *HSI2*- or *MED13*-overexpressing plants display the opposite phenotypes. The overexpression phenotypes of *HSI2* and *MED13* are abolished in *med13* and *hsi2 hsl1*, respectively, indicating that HSI2 and MED13 together are required for these functions. The HSI2 C-terminal region interacts with HDA6, whose overexpression also reduces seed maturation gene expression and lipid accumulation. Moreover, HSI2, MED13 and HDA6 bind to the proximal promoter and 5′-coding regions of seed maturation genes. Taken together, our results suggest that HSI2 recruits MED13 and HDA6 to suppress directly a subset of seed maturation genes post-germination.**

**Keywords:** Arabidopsis • Embryogenesis • Gene expression • MEDIATOR • Seed maturation genes.

**Abbreviations:** BiFC, bimolecular fluorescence complementation; ChIP, chromatin immunoprecipitation; Co-IP, co-immunoprecipitation; EAR, ERF-associated amphiphilic repression; GFP, green fluorescent protein; GST, glutathione S-trasnsferase; GUS, β-glucuronidase; HDA6, HISTONE DEACETYLASE 6; HSI2, HIGH-LEVEL EXPRESSION OF SUGAR-INDUCIBLE GENE 2; HSL1, HSI2-like; MED, MEDIATOR; Pol II, RNA polymerase II; qPCR, quantitative PCR; RNAi, RNA interference; WT, wild type; YFP, yellow fluorescent protein.

## Introduction

During seed development, plant embryogenesis is typically divided into two phases, morphogenetic and maturation. The morphogenetic process generates embryonic cell types, tissues and organs, whereas the maturation process comprises a series of events to ensure that the fully developed embryo accumulates a sufficient amount of storage reserves, becomes desiccated and finally assumes a metabolically quiescent state (West and Harada 1993, Goldberg et al. 1994). At least four regulatory genes are involved in establishing the seed maturation program (Suzuki and McCarty 2008): *LEAFY COTYLEDON 1* (*LEC1*), which encodes the HAP3 subunit of the CCAAT box-binding factor (Lotan et al. 1998), and *ABSCISIC ACID-INSENSITIVE 3* (*ABI3*), *FUSCA3* (*FUS3*) and *LEC2* which code for plant-specific transcription factors sharing a conserved B3 DNA-binding domain (Luerben et al. 1998, Stone et al. 2001, Finkelstein et al. 2008). *LEC1* and *ABI3*/*FUS3*/*LEC2* (*AFL*) genes function in a complex regulatory network culminating in the activation of a set of largely overlapping downstream genes including those encoding transcription factors and enzymes for starch and lipid biosynthesis (Holdsworth et al. 2008, Suzuki and McCarty 2008).

Under appropriate conditions, the seed germinates and develops into a seedling using as an energy source products derived from degradation of storage reserves (Theodoulou and Eastmond 2012). During the dormant to vegetative phase transition, two repressors, HIGH-LEVEL EXPRESSION OF SUGAR-INDUCIBLE GENE 2 (HSI2) and HSI2-like 1 (HSL1) (Tsukagoshi et al. 2005, Tsukagoshi et al. 2007), are required to inhibit expression of seed maturation genes. Both repressors are B3 DNA-binding domain transcription factors with high sequence homology. Independently identified by Suzuki et al. (2007), HSI2 and HSL1 have also been referred to as VP1/ABI3-Like1 (VAL1) and VAL2, respectively. *HSI2* and *HSL1* transcript levels are induced upon germination and they peak at 5 d after germination (Tsukagoshi et al. 2005, Tsukagoshi et al. 2007). Expression levels of a number of target genes which are moderately

*Plant Cell Physiol.* 0(0): 1–18 doi:10.1093/pcp/pcw095, Advance Access publication on 11 May 2016, available online at www.pcp.oxfordjournals.org

derepressed in the *hsi2* mutant become further elevated in the *hsi2 hsl1* (called *KK*) double mutant (Suzuki et al. 2007, Tsukagoshi et al. 2007). Therefore, the two factors are functionally redundant and both are required to restrain fully recapitulation of the seed maturation program in early seedling growth (Holdsworth et al. 2008, Suzuki and McCarty 2008). Consistent with their repressive capacity, both HSI2 and HSL1 carry a sequence similar to the ERF-associated amphiphilic repression (EAR) motif, which is required for their inhibitory function (Tsukagoshi et al. 2005, Tsukagoshi et al. 2007).

In eukaryotes, the regulatory functions of DNA-bound transcription factors are communicated to the RNA polymerase II (Pol II) transcription machinery via a conserved, multiprotein complex called MEDIATOR (MED). First identified in yeast and subsequently in mammalian cells, the MED complex is comprised of at least 30 subunits (Flanagan et al. 1991, Koleske and Young 1994, Conaway et al. 2005, Kornberg 2005, Malik and Roeder 2005, Beyer et al. 2007). The yeast MED complex is made up of four subdomains, i.e. the head, middle, tail and a separable kinase domain called the CDK8 module (Asturias et al. 1999, Davis et al. 2002). Although both positive and negative transcription regulatory functions have been assigned to MED complex subunits (Poss et al. 2013), the CDK8 module is known to be largely but not exclusively responsible for transcriptional repression (Poss et al. 2013). For example, MED12, a CDK8 module subunit, associates with the repressive histone methyltransferase G9a to suppress neuronal genes in non-neuronal cells (Ding et al. 2008). Two other subunits of the human CDK8 module, CDK8 and CDK19, act as transcriptional repressors by recruiting protein arginine methyltranferase 5 (PRMT5) to suppress target gene expression through symmetric dimethylation of histone H4 arginine 3 (H4R3me2s) (Tsutsui et al. 2013).

Purified Arabidopsis MED complex contains 21 conserved and six plant-specific subunits (Bäckström et al. 2007). Although homologs of the CDK8 module subunits were not found in the biochemically purified complex, subsequent bioinformatics analysis uncovered Arabidopsis genes encoding these subunits; MED12, MED13, CDK8, CYC1;1 and CYC1;2 are indeed present in the Arabidopsis genome (Gillmor et al. 2010, Ito et al. 2011). The functions of >10 Arabidopsis MED subunits have been studied so far, and, not surprisingly, they have been found to play roles in growth and development and hormonal signaling. For example, STRUWWELPETER (SWP), a homolog of MED14, is involved in regulating leaf cell proliferation (Autran et al. 2002), whereas Non-Recognition-of BTH4 (NRB4), an ortholog of MED15, has been implicated in salicylic acid signaling (Canet et al. 2012). Initially characterized as a positive regulator of *FLOWERING LOCUS T* (Cerdán and Chory 2003), PHYTOCHROME AND FLOWERING TIME 1 (PFT1) was subsequently identified as MED25 (Bäckström et al. 2007). MED12 and MED13, subunits of the CDK8 module, have been shown to modulate embryo patterning in Arabidopsis (Gillmor et al. 2010), and mutations in *MACCHIBOU 2* (*MAB2*), also known as *MED13*, cause cell division defects in embryos (Ito et al. 2011), suggesting that MED13 is required for proper cell division during embryogenesis. A recent study also suggests that MED12 and MED13 act as global regulators of developmental timing by fine-tuning the expression of temporal regulatory genes (Gillmor et al. 2014).

In addition to MED subunits, transcriptional repressors may also recruit histone modification enzymes to modify chromatin marks on target gene loci. Indeed, Zhou et al. (2013) have recently shown that repression of seed maturation genes by HSL1 is mediated in part by its interaction with HISTONE DEACETYLASE 19 (HDA19) (Zhou et al. 2013). The HSL1/HDA19 association is surprisingly specific, as the HSL1 homolog, HSI2, does not bind to HDA19 (Zhou et al. 2013).

Here, we investigated how the negative regulatory function of HSI2 is communicated to the MED complex to repress transcription. We found that both HSI2 and HSL1 interacted with the MED13 subunit of the CDK8 module. MED13 deficiency led to enhanced expression of seed maturation genes as well as accumulation of lipids in cotyledons. In contrast, overexpression of *MED13* suppressed seed maturation gene expression and decreased lipid accumulation. In addition, HSI2 also specifically associated with HISTONE DEACETYLASE 6 (HDA6) but not HDA19. Chromatin immunoprecipitation (ChIP) experiments showed direct binding of HSI2, MED13 and HDA6 to promoter and 5′-coding regions of a set of seed maturation genes. Furthermore, binding of MED13 and HDA6 to seed maturation genes was dependent on HSI2. Taken together, our results suggest that HSI2 recruits MED13 and HDA6 to regulate embryonic traits in Arabidopsis cotyledons.

## Results

### HSI2 represses fatty acid biosynthesis and seed maturation gene expression

Seedlings of the *hsi2 hsl1* (*KK*) double mutant have been shown to accumulate lipid droplets in hypocotyls and cotyledons, suggesting that HSI2 and HSL1 may repress lipid biosynthesis in seedlings. Here, we chose to focus on HSI2 because this factor was initially isolated as an active transcriptional repressor with a B3 DNA-binding domain (Tsukagoshi et al. 2005). Moroever, interacting proteins of HSL have recently been characterized (Zhou et al 2013). To provide direct evidence for the repressive function of *HSI2*, we generated transgenic plants overexpressing this gene. **Supplementary Fig. S1A** confirms a previous report that total fatty acid levels in *hsi2 hsl1* (*KK*) double mutant seedlings were >2-fold higher than wild-type (WT) levels (Tsukagoshi et al. 2007). In contrast, *35S:HSI2*-overexpressing seedlings produced <50% of the WT fatty acid levels. Comparative transcript analysis of a set of seven seed maturation genes (*LEC1*, *LEC2*, *WRI1*, *FUS3*, *Ole3*, *At2S3* and *ABI3*) in cotyledons of various genotypes confirmed up-regulation and repression of all seven genes in the double mutant *KK* (Tsukagoshi et al. 2007) and in *35S:HSI2*, respectively (**Supplementary Fig. S1B**). We also found that *HSL1* overexpression was able to suppress expression of seed maturation genes, confirming its repressive function (**Supplementary Fig. S1C**).

## HSI2 self-interacts and also binds to HSL1

Because most transcription factors bind to target DNA sequences as a dimer (Amoutzias et al. 2008), we examined by a bimolecular fluorescence complementation (BiFC) and co-immunoprecipitation (Co-IP) experiment whether HSI2 has this property. **Fig. 1** shows that HSI2 could indeed self-interact with the interaction signal mainly localized to the nucleus. This interaction was confirmed by Co-IP analysis when the proteins were transiently expressed in *Nicotiana benthamiana* leaves (**Fig. 1C**). In addition, HSL1 was able to self-interact (**Fig. 1B, C**) and also to associate with HSI2 (**Supplementary Fig. S2**).

## HSI2 interacts with MED13 in vitro and in vivo

The repressor function of HSI2 (Tsukagoshi et al. 2005) prompted us to test its possible interaction with the CDK8 module. We first tested if HSI2 would interact with MED13 by in vitro pull-down experiments. Because of its large size, we divided the MED13 protein into three fragments and interrogated their binding capacity separately. **Fig. 2** shows that HSI2 associated with the 103 amino acid TRAP240 fragment (amino acids 1,058–1,160). No HSI2 interaction was seen with either the MED13 N-terminal (amino acids 1–1,057) or C-terminal fragment (amino acids 1,161–1,877) (**Fig. 2C**). Further dissection of HSI2 showed that the TRAP240 fragment interacted with the N-terminal region (amino acids 1–470) of HSI2, although a weak association was also seen with the C-terminal region (amino acids 461–789) (**Fig. 2E**). BiFC and Co-IP assays further confirmed HSI2–TRAP240 interaction in vivo (**Fig. 2F, G**). Similar experiments showed that HSL1 also bound to the TRAP240 domain of MED13 (**Supplementary Fig. S3**).

## Expression profile of the *MED13* promoter

We generated 26 independent transgenic lines expressing *MED13:GUS* (β-glucuronidase) and analyzed several representative lines in detail. Histochemical staining revealed that *MED13:GUS* was expressed in seeds and germinating seedlings 1 d after imbibition. In 3-day-old seedlings, GUS expression became stronger in cotyledons (**Supplementary Fig. S4A–C**). Furthermore, in 10-day-old seedlings, strong GUS expression was observed in cotyledons, petioles and hypocotyls (**Supplementary Fig. S4D**). GUS expression still persisted in rosette leaves until the flowering stage (**Supplementary Fig. S4F**). GUS staining was also observed in root tips, flowers and siliques (**Supplementary Fig. S4E, G–H**). *MED13* expression levels in rosette leaves, roots, flowers, siliques and seeds were further confirmed by quantitative PCR (qPCR) (**Supplementary Fig. S6A**).

We also used a *MED13-GFP* (green fluorescent protein) line under the control of a native *MED13* promoter to examine the *MED13* expression pattern during embryogenesis. *MED13* was expressed in early globular embryos and the peripheral endosperm (**Supplementary Fig. S4I**), and the expression became stronger and extended to the whole embryo at the heart, the cotyledon-curling and the late maturation stage (**Supplementary Fig. S4J–L**). These expression results suggest a role for *MED13* in embryogenesis.

## Mutations in *MED13/MAB2/GCT2* display a variety of phenotypes

*MED13* (*MAB2* or *GCT2*) has been previously shown to be important in embryogenesis and early plant development. Disruption of *MED13* (*MAB2*) function led to abnormal cell division and caused defects in cotyledon development (Ito et al. 2011). An ethyl methanesulfonate- (EMS) induced mutation, *gct2*, which causes a *MED13* functional deficiency, also showed embryo patterning abnormality (Gillmor et al. 2010). To understand more about MED13 function, we selected two mutants in the *MED13/MAB2/GCT2* genomic locus including *gct2* and a T-DNA insertion line, Salk_018056 (Alonso et al. 2003); these mutant alleles were renamed *med13-1* (*gct2*) and *med13-2* (Salk_018056) (**Supplementary S5A**). Both mutant alleles produced a variety of phenotypic defects. Among plants with the *med13/med13* genotype, only about 25% of the mutant seedlings displayed cotyledon defects, whereas about 75% showed WT-like cotyledons (**Table 1**; **Supplementary Fig. S5**). We classified cotyledon phenotypes into three groups (I–III) depending on the phenotypic severity (**Supplementary Fig. S5D–F, I–K**). Group I plants showed mildly fused cotyledons which were twisted and narrow (**Supplementary Fig. S5D, I**). This group accounted for 4.22% ($n = 340$) for *med13-1* and 3.37% ($n = 385$) for *med13-2* of the total heterozygous population (**Table 1**). Under our growth conditions, only 25% for *med13-1* ($n = 14$) and 30% for *med13-2* ($n = 13$) of Group I seedlings could survive until the flowering stage when transferred to soil. Most of the mutant plants became arrested in growth after a week of growth on soil (**Supplementary Fig. S6B**). Group II mutants displayed strongly fused cotyledons, with one being shorter or smaller and the other longer or larger with a heart-shaped phenotype (**Supplementary Fig. S5E, J**). Occasionally, both *med13-1* and *med13-2* seedlings showed the heart-shaped phenotype on both cotyledons (**Supplementary Fig. S7B, C**). The segregation of *med13-1* and *med13-2* was 1.81% ($n = 340$) and 1.24% ($n = 385$), respectively (**Table 1**). The mutants in Group III showed very strong cotyledon fusion leading to a single cotyledon and developing cup-shaped phenotype (**Supplementary Fig. S5F, K**). The segregation for *med13-1* and *med13-2* in this group was 0.4% ($n = 340$) and 0.35% ($n = 385$), respectively. Neither *med13-1* nor *med13-2* seedlings in Group II and Group III could survive until the flowering stage.

To investigate further the low frequency of mutant phenotype segregation, we used RNA interference (RNAi) to knock down *MED13* expression. Among the transgenic RNAi lines, about 30% displayed aberrant cotyledons ($n = 125$), whereas about 70% developed normal cotyledons although the RNAi seedlings were slightly smaller than WT seedlings (**Supplementary Fig. S8A**). Seedlings with abnormal cotyledons died 2 weeks after transfer to soil. However, transgenic plants with normal cotyledons survived and produced seeds as WT plants. We germinated transgenic seeds and analyzed the *MED13* transcript in these knockdown seedlings.

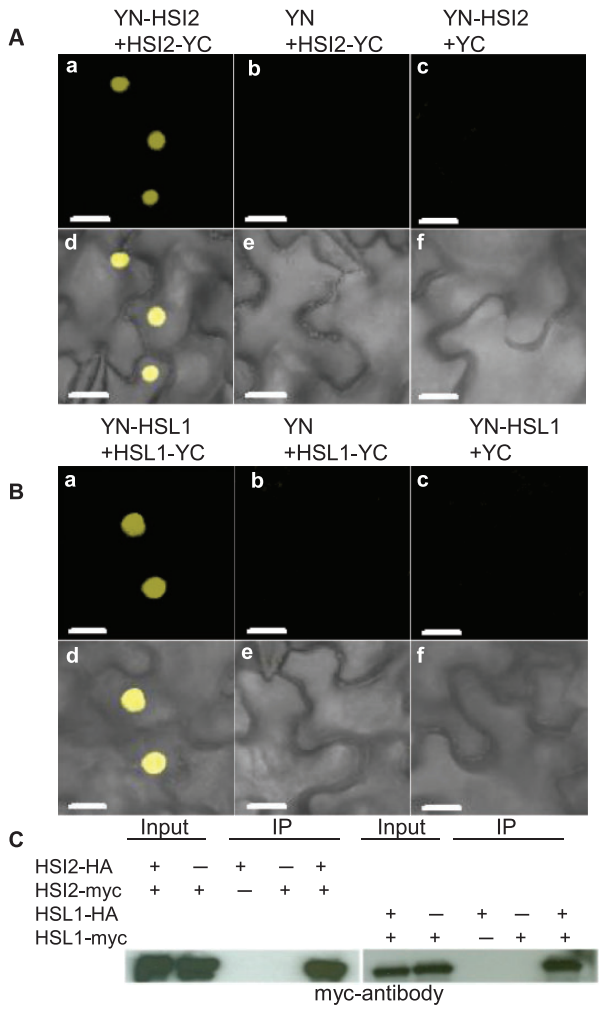


**Fig. 1** Self-association of HSI2 and HSL1. BiFC analysis of HSI2/HSI2 (A) and HSL1/HSL1 (B) interaction in *N. benthamiana* leaf cells. The N-terminal region of EYFP was fused to full-length HSI2 or HSL1 (YN–HSI2 or YN–HSL1) and the C-terminal region of EYFP to HSI2 or HSL1 (HSI2–YC or HSL1–YC) (a). Empty plasmid containing YN–YFP or YFP–YC was used as a negative control (b and c). EYFP fluorescence (a–c) and EYFP fluorescence images merged with bright-field images (d–f). (C) Co-immunoprecipitation (Co-IP) showing self-interaction of HSI2 and HSL1. Total protein was extracted from tobacco leaves co-expressing 35S:HSI2-HA and 35S:HSI2-myc, 35S:HSL1-HA and 35S:HSL1-myc, only 35S:HSI2-myc or only 35S:HSL1-myc. HSI2-HA (the protein) was then immunoprecipitated with anti-HA antibody, and the immunoblot was detected with anti-myc antibody. Scale bar = 10 μm.

Notwithstanding their WT cotyledon phenotype, the transgenic seedling showed greatly reduced *MED13* transcript levels compared with the WT (**Supplementary Fig. S8B**). These results suggest that the low phenotypic manifestation of *med13* mutants is at least partially due to incomplete penetrance.

## *MED13* deficiency resulted in lipid accumulation in cotyledons

HSI2–MED13 interaction suggested that this MED subunit may regulate lipid accumulation as well. To investigate this possibility, we compared lipid contents in cotyledons of defective *med13-1* and *med13-2* seedlings and WT-like *med13/med13* seedlings with those of WT seedlings. **Fig. 3** shows that cotyledon-defective *med13-1* and *med13-2* seedlings showed strong Fat Red staining in cotyledons and slight staining in true leaves (**Fig. 3A–C**). Compared with WT seedlings, both mutants showed a greater number of lipid droplets in cotyledons when stained with Bodipy493/503 or Nile Red (**Fig. 3D–I**). Furthermore, strong lipid staining was observed in defective cotyledons (**Supplementary Fig. S7D–F**). Quantitative data showed that both cotyledon-defective *med13-1* and *med13-2* contained about a three times higher number of lipid droplets compared with the WT, irrespective of the lipid marker used (**Fig. 3J, K**).

Next, we compared fatty acid compositions in mutant and WT cotyledons. **Supplementary Fig. S9A** shows a significant increase in palmitic acid (C16:0) and linoleic acid (C18:2) in both *med13-1* and *med13-2* cotyledons compared with WT cotyledons. In contrast, both mutants produced less linolenic acid (C18:3) compared with the WT, although no significant difference was observed in the content of palmitoleic acid (C16:1), hexadecatrienoic acid (C16:3), stearic acid (C18:0) and oleic acid (C18:1). Total fatty acid content per mg fresh weight was 2–3 times higher in *med13-1* and *med13-2* compared with the WT (**Supplementary Fig. S9A**, inset). We also analyzed lipid staining and droplets in *med13/med13* cotyledons with WT phenotype. In agreement with their WT-like phenotype, these cotyledons showed no significant alteration in lipid accumulation (**Supplementary Fig. S10**). Moreover, there was no significant difference between these WT-like mutants and the WT in the expression of seed maturation genes in cotyledons, except that the *At2S3* transcript levels were higher in the WT-like mutants (**Supplementary Fig. S11**). These results suggest that MED13 negatively regulates lipid accumulation in Arabidopsis cotyledons.

## Seedlings of *med13* mutant alleles showed severe growth defects without sucrose

The increased lipid contents in *med13* cotyledons as well as plant growth arrest after being transferred to soil (**Fig. 3**; **Supplementary Figs. S7, S9**) suggested that the breakdown of storage lipid to sugar may be impaired in mutants during seed germination and seedling establishment. Therefore, we tested if sucrose addition could improve seedling growth. On minimal medium, *med13-1* and *med13-2* seedlings were small with a significantly shorter root and hypocotyl, and greatly reduced fresh weight compared with WT seedlings (**Supplementary Fig. S12**). With sucrose, however, both mutant seedlings showed an increase in hypocotyl length and fresh weight, although the root length was still shorter than in the WT (**Supplementary Fig. S12**). Notably, sucrose addition did not rescue the defective cotyledon phenotype in mutant seedlings. Moreover, sucrose was not responsible for the incomplete penetrance in the mutants because the frequency of mutant phenotypes was not changed by sucrose (**Supplementary Table S1**).

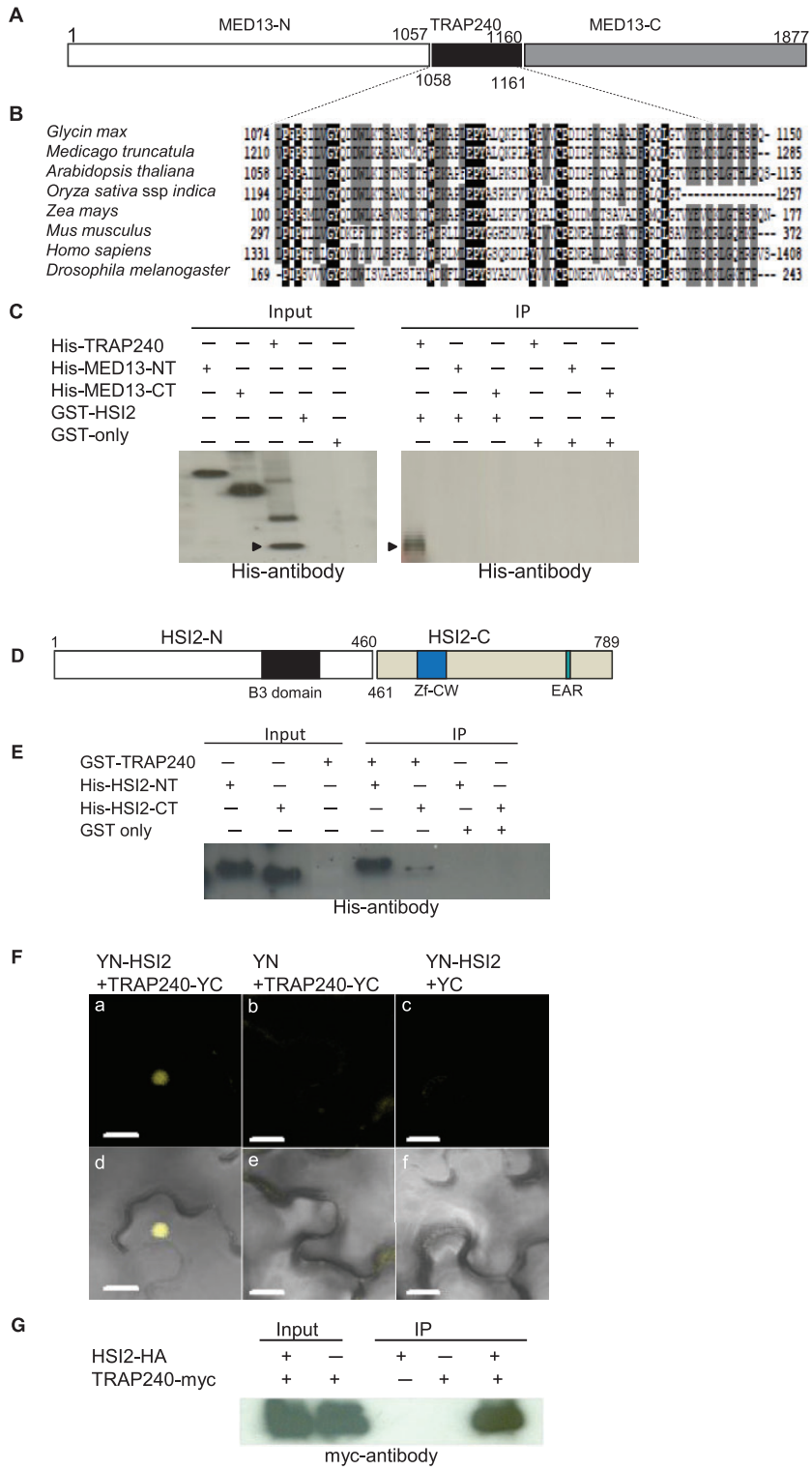


**Fig. 2** HSI2 interacts with the TRAP240 domain of MED13. (A) Schematic diagram of MED13 protein structure which is divided into an N-terminal region (amino acids 1–1,057), a TRAP240 domain (amino acids 1,058–1,160) and a C-terminal region (amino acids 1,161–1,877). (B) Sequence alignment of TRAP240 domains of AtMED13, OsMED13, GmMED13, MtMED13, ZmMED13, MmMED13, HsMED13 and DmMED13. Black highlighted letters indicate identical residues, whereas gray represent similar residues. (C) Pull-down assay showing interaction of the TRAP240 domain of MED13 with HSI2. Arrowheads indicate the His-TRAP240 domain. (D) Schematic diagram showing N-terminal (amino acids 1–460) and C-terminal (amino acids 461–789) region of the HSI2 protein. The black box represents the B3 DNA-binding domain, the blue box indicates the CW-type zinc finger (Zf-CW) and the green box depicts the EAR motif. (E) Pull-down assay showing the interaction of TRAP240 with the N-terminal region of HSI2. (F) BiFC analysis of HSI2–TRAP240 interaction in *N. benthamiana* leaf cells. The N-terminal region of EYFP

(continued)

## Enhanced expression of seed maturation genes in *med13* cotyledons

The enhanced lipid content in cotyledons of *med13* mutant alleles may be due to inappropriate expression of seed maturation genes such as *LEC1*, *LEC2*, *WRI1*, *FUS3*, *Ole3*, *At2S3* and *ABI3* (Guerche et al. 1990, Namabara et al. 1992, Lotan et al. 1998, Stone et al. 2001, Kroj et al. 2003, Siloto et al. 2006, Maeo et al. 2009). To investigate this possibility, we compared expression levels of these genes between cotyledons of mutants and the WT by real-time qPCR. **Fig. 4** shows that although *LEC2* and *WRI1* mRNA levels were slightly increased (but significantly different), expression levels of *LEC1*, *At2S3*, *FUS3*, *Ole3* and *ABI3* were highly elevated (30- to 2,000-fold) in cotyledons of both *med13* alleles compared with WT cotyledons (**Fig. 4A**). Expression of seed maturation genes was also increased in cotyledons of the double mutant *KK*. Consistent with the *med13* results, plants overexpressing *MED13* showed a reduction in both lipid accumulation and transcript levels of seed maturation genes (**Fig. 4B**; **Supplementary Fig. S9C**). We also observed that expression levels of *TAG1*, which is directly involved in triacylglyerol assembly in the endoplasmic reticulum (Ohlrogge and Browse 1995), were elevated in both *med13* alleles and the double mutant *KK* (**Supplementary Fig. S7G**). These results show that MED13 negatively regulates lipid accumulation and is required to suppress seed maturation genes during seed germination and seedling establishment.

## MED13 protein localizes to the nucleus

We examined transient expression of a *ProMED13:MED13-GFP* or a *Cauliflower mosaic virus* (CaMV) 35S promoter (*Pro35S:MED13-GFP*) construct in tobacco epidermal cells. MED13–GFP fusion protein was localized in the nucleus irrespective of the promoter used (**Supplementary Fig. S13**), suggesting a nuclear function of MED13.

## HSI2 specifically interacts with HDA6

Zhou et al. (2013) reported that HSL1 recruits HDA19 to repress seed maturation by direct binding to chromatin on the promoter and/or coding region of seed maturation genes (Zhou et al. 2013). More importantly, they found no interaction between HSI2 and HDA19, suggesting high specificity. The high homology between HDA19 and HDA6 (http://www.arabidopsis.org/cgi-bin/wublast/wublast) prompted us to test for possible HSI2–HDA6 interaction. **Fig. 5** shows that when purified His-HSI2 (N- or C-terminal region of HSI2) recombinant protein was incubated with glutathione *S*-transferase (GST)–HDA6 protein, HDA6–GST was pulled down by either His-HSI2 (N-terminus) or His-HSI2 (C-terminus). Furthermore, the C-terminal region of HSI2 which includes the repressive motif (EAR) showed strong interaction with HDA6 (**Fig. 5A**).

The HSI2–HDA6 interaction was further confirmed in vivo using BiFC analysis. **Fig. 5B** (a, d) shows that nuclear signal was observed when YN–HSI2 and HDA6–YC were co-expressed in tobacco (*N. benthamiana*) leaf cells. In contrast, no nuclear signal was detected when either YN–HSI2 or HDA6–YC was expressed with an empty plasmid which was used as a negative control (**Fig. 5B**, b and c, e and f). The HSI2–HDA6 interaction was also confirmed by Co-IP analysis (**Fig. 5C**). In addition, no interaction was found between YN–HSL1 and HDA6–YC, and we also confirmed that HSL1 can associate with HDA19 as reported by Zhou et al. (2013) (**Supplementary Fig. S14**). These results indicate that HSI2, but not HSL1, interacts with HDA6 in the nucleus.

Next, we investigated whether the EAR motif of HSI2-CT mediates the HSI2–HDA6 interaction by BiFC analysis. The removal of the EAR motif (HSI2-CT-ΔEAR) did not affect the HSI2–HDA6 interaction (**Supplementary Fig. S15C**, **b** and **e**) but the interaction was disrupted by Zf-CW domain deletion (**Supplementary Fig. S15C**, **c** and **f**). These results suggest that the Zf-CW domain is needed for HSI2–HDA6 association. To identify HDA6 sequences responsible for the interaction, we divided the protein into three fragments: D1, histone deacetylase domain (HD) and D2 (**Supplementary Fig. S15A**). Interaction was observed only between D2 of HDA6 with HSI2-CT (**Supplementary Fig. S15D**, **g–l**).

**Table 1** Frequency of mutant phenotypes in the presence of sucrose

| Genotype (*n*) | WT (%) | WT-like | Group I | Group II | Group III | Total |
|---|---|---|---|---|---|---|
| | (+/+)/(+/−) | (−/−) | (−/−) | (−/−) | (−/−) | |
| *Med13-1* (+/−) (340)[a] | 80.67 | 12.90 | 4.22 | 1.81 | 0.40 | 19.33 (33)[b] |
| **Med13-2** (+/−) (385)[a] | 77.37 | 17.67 | 3.37 | 1.24 | 0.35 | 22.63 (22)[b] |

The requency of seedling phenotype was observed by scoring 12- to 14-day-old seedlings derived from a heterozygous population of *Med13* (+/−) mutants grown on MS medium supplemented with 1% sucrose for further growth and genotyping.
[a] The number of genotyped seedlings.
[b] The percentage of cotyledon-defective mutants.

**Fig. 2** Continued
was fused to full-length HSI2 (YN–HSI2) and the C-terminal region of EYFP to TRAP240 (TRAP240–YC) (a). Empty plasmid containing YN–YFP or YFP–YC was used as a negative control (b and c). EYFP fluorescence (a–c), and EYFP fluorescence images were merged with bright field images (d–f). (G) Co-IP assay showing HSI2–TRAP240 interaction. Total protein was extracted from tobacco leaves co-expressing 35S:HSI2-HA and 35S:TRAP240-myc or only 35S:HSI2-HA or only 35S:TRAP240-myc. HSI2-HA (the proteins) were immunoprecipitated with anti-HA antibody and the immunoblot was detected with anti-myc antibody. Scale bar = 10 μm.

## Overexpression of HDA6 reduces lipid accumulation and down-regulates seed maturation genes in cotyledons

The binding of HSI2 to HDA6 implicates the latter in repressing seed maturation genes. To investigate this issue further, we first determined lipid accumulation in cotyledons of *axe1-5* (a *hda6* allele) (Murfett et al. 2001), knock-down line *HDA6* RNAi (in Col-0 background) and *35S:HDA6*-overexpressing plants. We found that total fatty acid content in cotyledons deficient in HDA6 (*axe1-5* and *HDA6* RNAi lines) was significantly higher than that in the WT control, whereas the opposite results were

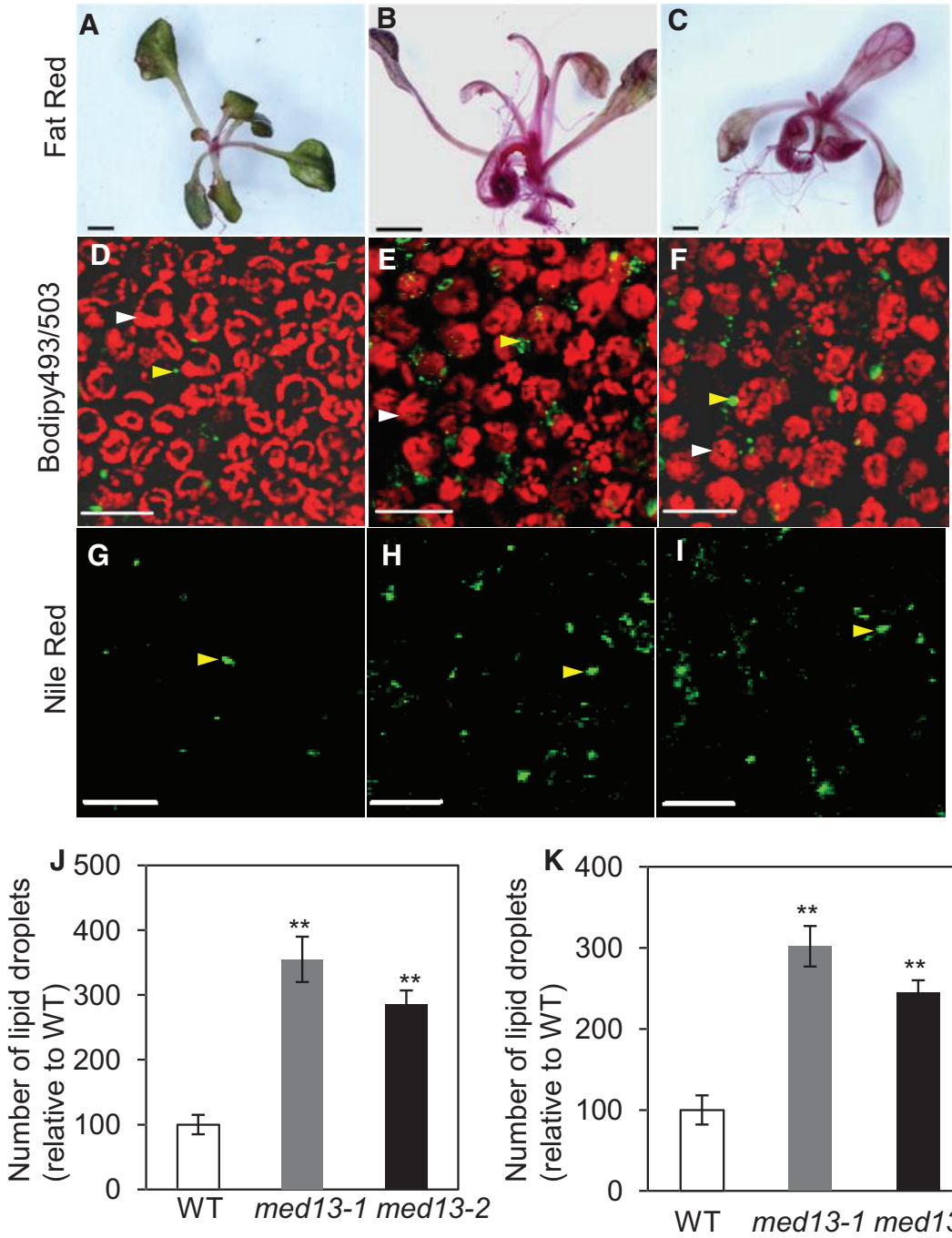


**Fig. 3** Enhanced lipid accumulation in cotyledons of *med13* mutants. Twelve-day-old seedlings of WT (A, D, G), *med13-1* (B, E, H) and *med13-2* (C, F, I) stained with Fat Red marker (A–C), Bodipy 493/503 marker (D–F) or Nile Red marker (G–I), respectively. (J) and (K) represent quantitative data with three biological replicates showing a number of lipid droplets in *med13* mutants relative to the WT. The number of lipid droplets was counted per image of the selected area of 40,000 $\mu m^2$ observed in cotyledons. Yellow and white arrowheads indicate lipid droplets and chloroplasts, respectively. Average values ± SE ($n$ = 3) are given. ** Indicate significantly different from the WT at the 1% level ($P < 0.01$). Scale bar = 1 mm (A–C), 50 μm (D–I).

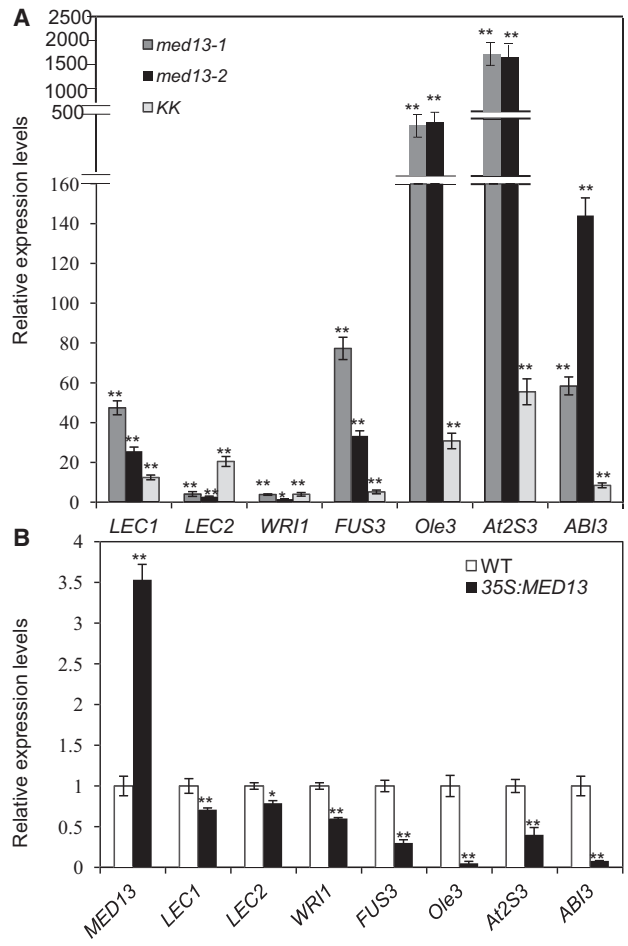


**Fig. 4** MED13 is required to repress expression of seed maturation genes. (A and B) Transcript levels of seed maturation genes in *med13* mutant and *KK* double mutant seedlings (A), and the *35S:MED13*-overexpressing line (B). Total RNA was collected from cotyledons of 10- to 14-day-old seedlings grown with 1% sucrose. The expression level was presented relative to that in the WT which was set as 1. Average values ± SE ($n > 6$) are given. * and ** indicate significantly different from the WT at 5% ($P < 0.05$) and 1% ($P < 0.01$), respectively.

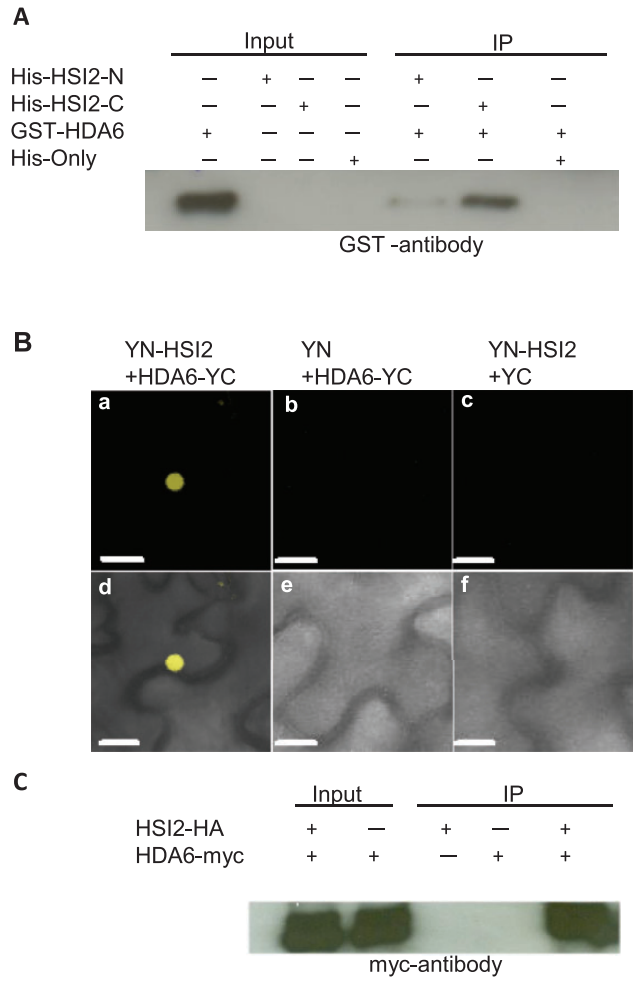


**Fig. 5** HSI2 interacts with HDA6 in vitro and vivo. (A) In vitro pull-down assay showing interaction of HDA6 with the C-terminal region of HSI2. (B) BiFC analysis of HDA6–HSI2 interaction in *N. benthamiana* leaf cells. The N-terminal region of EYFP was fused to full-length HSI2 (YN–HSI2) and the C-terminal region of EYFP to HDA6 (HDA6–YC) (a). Empty plasmid containing YN–YFP or YFP–YC was used as a negative control (b and c). EYFP fluorescence (a–c), and EYFP fluorescence images merged with bright-field images (d–f). (C) Co-immunoprecipitation assay showing HSI2–HDA6 interaction. Total protein was extracted from tobacco leaves co-expressing 35S:HSI2-HA and 35S:HDA6-myc, only 35S:HSI2-HA or only 35S:HDA6-myc. HSI2-HA (the proteins) were immunoprecipitated with anti-HA antibody and the immunoblot was detected with anti-myc antibody. Scale bar = 10 μm.

found in cotyledons of *35S:HDA6* seedlings (**Supplementary Fig. S16A**). Comparative transcript analysis showed that expression levels of *LEC1*, *LEC2*, *WRI1*, *FUS3*, *Ole3*, *At2S3* and *ABI3* were significantly reduced in the *35S:HDA6* line (**Supplementary Fig. S16B**). These results show that HDA6 is also a key repressor of lipid biosynthesis and seed maturation genes in Arabidopsis cotyledons.

## Overexpression of *MED13* or *HSI2* cannot rescue phenotypic defects in the *KK* double mutant or *med13* mutant, respectively

Our results so far showed that MED13 and HSI2 can act as repressors of the seed maturation program and negatively regulate lipid accumulation in cotyledons (**Fig. 4**; **Supplementary Fig. S1**). Because the TRAP240 domain of MED13 protein interacted with HSI2 in vitro and vivo, it is likely that the two proteins form a complex that is required to regulate lipid biosynthesis. To test this hypothesis, we expressed *MED13* in the *KK* double mutant and *HSI2* in the *med13* mutant to test for possible rescue of the defect and alteration of seed maturation gene expression.

**Fig. 6** shows that expression of *35S:HSI2* in *med13-2* and of *35S:MED13* in the double mutant *KK* was not able to complement the mutant phenotype observed in *med13-2* and *KK* mutants, respectively (**Fig. 6C, F**). Note that expression of *HSI2* or *MED13* in the WT (Col-0) did not alter cotyledon morphology (**Fig. 6B, E**). Consistent with this observation, in *med13-2* seedlings expressing *35S:HSI2* or in *KK* mutant

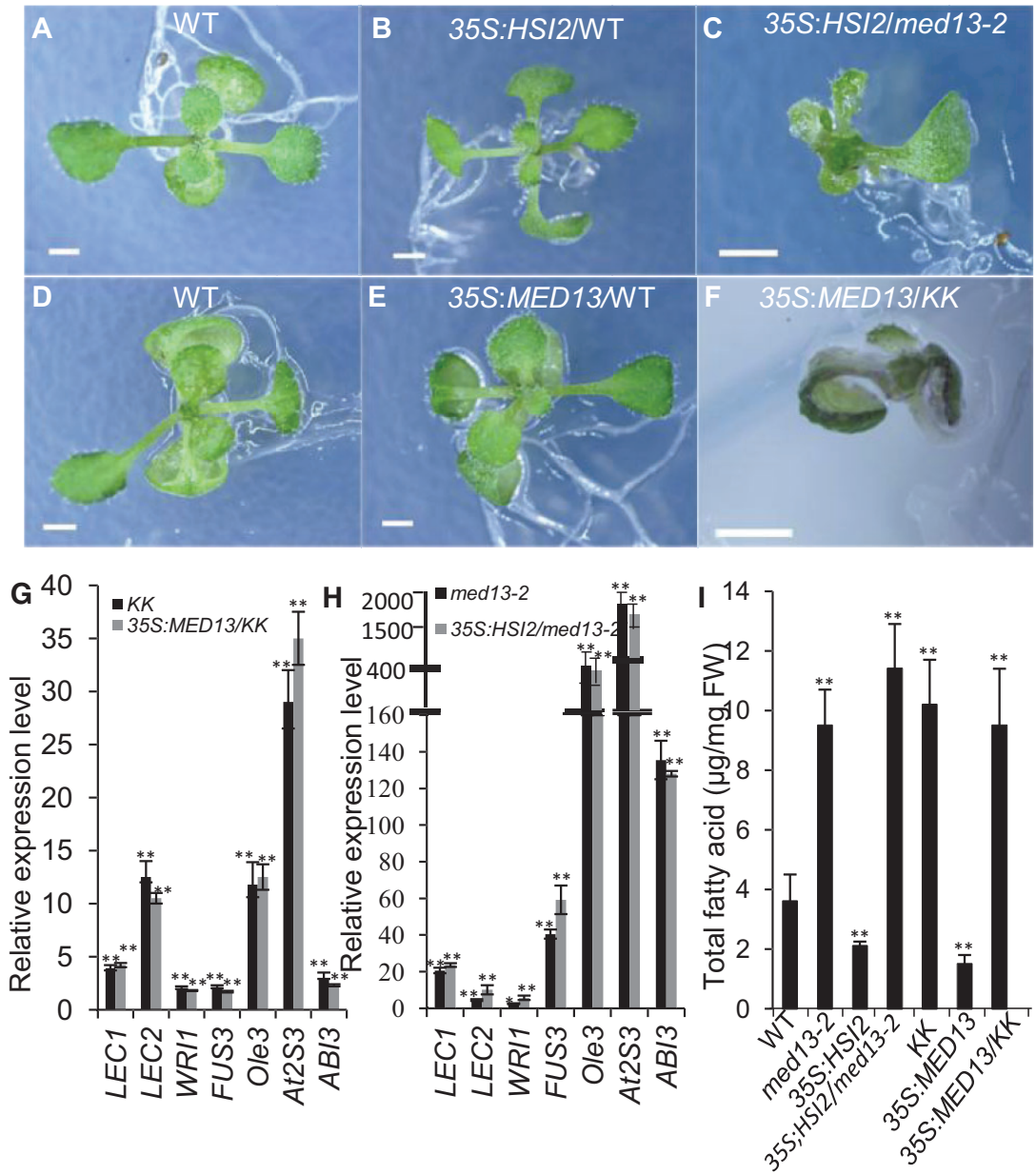


**Fig. 6** Both MED13 and HSI2 are required to repress expression of seed maturation genes. Two-week-old seedlings of (A) the WT, (B) *35S:HSI2* in the WT background and (C) *35S:HSI2* in the *med13-2* mutant background (*35S:HSI2/med13-2*). (D) The WT, (E) *35S:MED13* in the WT background and (F) *35S:MED13* in the *hsi2 hsl1* (*KK*) double mutant background (*35S:MED13/KK*). (G and H) Relative expression level of seed maturation genes in (G) a *35S:HSI2/med13-2* plant or (H) a *35S:MED13/KK* plant. (I) Total fatty acid extracted from cotyledons of 2-week-old plants of *35S:HSI2/med13-2* and *35S:MED13/KK*. For (G–I), average values ± SE ($n > 3$) are given. * and ** represent significantly different from the WT at 5% ($P < 0.05$) and 1% ($P < 0.01$), respectively. Scale bar = 1 mm.

seedlings expressing *35S:MED13*, transcription levels of seed maturation genes and cotyledon lipid accumulation still remained significantly higher than those of the WT (**Fig. 6G-I**). Since *med13* mutants show incomplete penetrance, we noted that expression of *HSI2* in *med13-2* (+/−) did not alter the phenotypic defect in *med13-2* seedlings which were segregated into WT-like *med13-2*, *med13-2* Group I, *med13-2* Group II and *med13-2* Group III (**Supplementary Fig. S17**). These results suggest that the negative regulatory function of HSI2 requires MED13, and vice versa. These two proteins probably function as a complex in the same pathway to modulate lipid repression.

## MED13, HSI2 and HDA6 directly bind to selective seed maturation genes

Cotyledons of *med13* mutant alleles and those of *MED13* overexpression seedlings showed the opposite molecular phenotype with respect to embryonic traits (**Figs. 3**, **4**), and similar results were obtained with the *KK* double mutant and *HSI2*

overexpression seedlings (**Supplementary Fig. S1**). One possibility is that MED13 and HSI2 may directly target genomic loci of at least selective seed maturation genes. Therefore, we generated transgenic plants (in the WT background) harboring *MED13-GFP* expressed from a native *MED13* promoter (*ProMED13:MED13-GFP*) and transgenic plants expressing *35S: HSI2-3HA* (*Pro35S:HSI2-3HA*). ChIP assays were performed to investigate the enrichment of MED13 or HSI2 on several genomic regions of four key seed maturation genes: *LEC1*, *LEC2*, *FUS3* and *ABI3*. To ensure the biological function of *ProMED13:MED13-GFP* and *35S:HSI2-HA*, we first transformed each of them into heterozygous plants carrying *med13-2* (+/−) or *hsi2 hsl1* (+/−), respectively. **Supplementary Fig. S18** shows that indeed *ProMED13:MED13-GFP* or *35S:HSI2-HA* was able to complement the respective mutant phenotype, suggesting that both constructs are functional. **Fig. 7B** (left-hand panel) shows that the *MED13* transcript level in *MED13-GFP* transgenic plants was about 2.0 times higher than in the WT. For ChIP analysis on target genes, we designed six primer regions including promoter region 1 (P1), P2 and P3, and coding/intron region 1 (C1), C2 and C3 (**Fig. 7A**). MED13 accumulation was enriched on the proximal promoter region P1 and coding region C1 of *LEC1*, *LEC2*, *FUS3* and *ABI3* but not in P2, P3, C2 and C3 regions (**Fig. 7C**). Control experiments showed no MED13 enrichment on the promoter and coding regions of *ACT7* (**Fig. 7E**).

**Fig. 7B** (right-hand panel) shows that *HSI2* transcript levels in *35S:HSI2-3HA* plants were 30 times greater than WT levels. Similar to the results with MED13, HSI2 enrichment was observed on the proximal promoter region of P1 and on the 5′-coding region of C1 of the *LEC1*, *LEC2*, *FUS3* and *ABI3* genes but not on P2, P3, C2 and C3 regions (**Fig. 7D**). There was no significant difference in HSI2 enrichment between WT and *35S:HSI2-3HA* plants on the *ACT7* genomic locus which was used as a negative control (**Fig. 7E**). Collectively, our findings show that MED13 and HSI2 directly bind to genomic loci of four key seed maturation genes.

We used a *hda6* complementation line (*HDA6/axe1-5*) (Earley et al. 2010) to investigate possible HDA6 association with chromatin of seed maturation genes. **Fig. 7E** shows that HDA6 was enriched on the promoter P1 and C1 5′-coding region of *LEC1*, *LEC2*, *FUS3* and *ABI3* but not on P2, P3, C2 and C3 regions.

## Binding of MED13 and HDA6 to seed maturation genes is dependent on HSI2

We examined whether binding of MED13 and HDA6 to key seed maturation genes (*LEC1*, *LEC2*, *FUS3* and *ABI3*) (**Fig. 7**) would require HSI2. We did not use the *MED13-GFP* transgenic line for these experiments because MED13 interacted with both HSI2 and HSL1. Therefore, we generated mouse antibody to MED13 and demonstrated its binding specificity by Western blot analysis of WT and *med13-2* mutant extracts (**Fig. 8B**) and used the antibody for ChIP experiments. Interestingly, we found that binding of MED13 to both promoter P1 and coding region C1 in *LEC*, *LEC2*, *FUS3* and *ABI3* was significantly reduced in the double mutant *KK* compared with the WT (**Fig. 8D**), suggesting that MED13 binding to seed maturation genes depends on HSI2 and HSL1. Next, we compared the enrichment of HDA6 between complemented line *ProHDA6:HDA6-Flag/axe1-5* (*HDA6/axe1-5*) and knockdown transgenic line *HSI2:RNAi* in the *ProHDA6:HDA6-Flag/axe1-5* background (*HSI2:RNAi/HDA6/axe1-5*). **Fig. 8C** shows the reduction of *HSI2* transcript in the *HSI2:RNAi/HDA6/axe1-5* background compared with the WT (Col-0) and the complemented line *HDA6/axe1-5*, but no significant difference in *HSI2* transcript level was found between the WT and the complemented line *HDA6/axe1-5* (**Fig. 8C**). ChIP assay with Flag antibody revealed that the HDA6 enrichment on both P1 and C1 was significantly reduced in *LEC1*, *LEC2*, *FUS3* and *ABI3* loci in the *HSI2:RNAi/HDA6/axe1-5* transgenic line compared with the complemented line *HDA6/axe1-5* (**Fig. 8E**). These results show that HDA6 binding to seed maturation genes is also dependent on HSI2.

## MED13, HSI2 and HDA6 repress histone acetylation

The down-regulation of seed maturation genes by overexpression of *MED13*, *HSI2* or *HDA6* prompted us to investigate possible altered histone modifications associated with seed maturation gene loci. Using *LEC1* and *LEC2* as representative genes, we observed histone modifications only on the proximal promoter P1 and 5′-coding region C1 of these two loci; these two regions serve as the binding sites of MED13, HSI2 or HDA6 (**Fig. 9A**). The histone H3 and H4 acetylation status on the P1 and C1 of these two genes was interrogated in transgenic plants carrying *35S:MED13*, *35S:HSI2* or *35S:HDA6*. All the three different transgenic lines contained significantly reduced H3ac and H4ac enrichment in P1 and C1 of *LEC1* and *LEC2* compared with the WT (**Fig. 9B, C**).

We next examined the enrichment of H3K9ac levels, which is associated with active plant gene expression (Ng et al. 2006). Consistent with the reduced enrichment of H3ac and H4ac, all the three different transgenic lines also showed reduced enrichment of H3K9ac in P1 and C1 of *LEC1* and *LEC2* (**Fig. 9B, C**). From these results, we conclude that the repression of seed maturation genes by *MED13*, *HSI2* or *HDA6* can be attributed in part to reduced accumulation of H3K9ac levels.

# Discussion

## A working model for regulation of seed maturation genes

The results presented here, along with previous observations of Zhou et al. (2013), are best explained by the working model in **Fig. 10**. According to this model, a HSI2 or HSL1 homocomplex or HSI2–HSL1 heterocomplex recognizes specific DNA sequences upstream of the promoter region of a subset of seed maturation genes (*LEC1*, *LEC 2*, etc). Upon binding to the *cis*-elements, these repressors recruit the MED13 subunit of the CDK8 module, thereby disrupting Pol II transcription. At the same time, HSL1 recruits HDA19 (Zhou et al. 2013) whereas HSI2 recruits HDA6 (this work) to erase positive histone marks (H3K9ac and H4Kac) on the proximal promoter and 5′-coding regions of the seed maturation gene. The deacetylation is

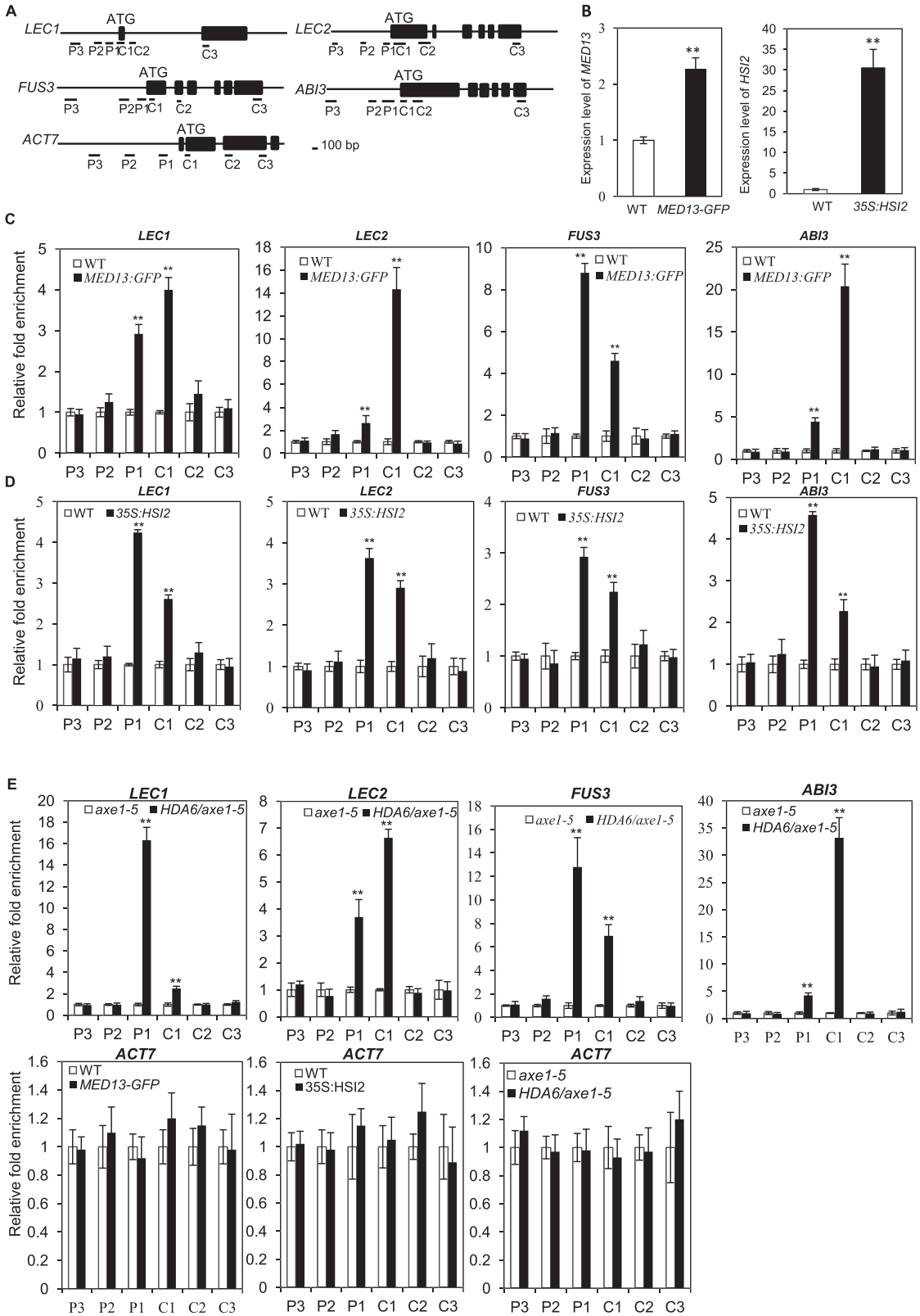


**Fig. 7** Binding of MED13, HSI2 and HDA6 to genomic loci of seed maturation genes. (A) Schematic representation of seed maturation genes. Genomic regions marked as P (promoter region) and C (coding or intron region) were interrogated by ChIP. (B) Expression levels of *MED13* or *HSI2* in WT and transgenic plants carrying *ProMED13:MED13-GFP* or *Pro35S:HSI2-HA*. (C–E) ChIP analysis of 2-week-old transgenic plants harboring *ProMED13:MED13-GFP* (C) and *Pro35S: HSI2-HA* (D), and *ProHDA6:HDA6-Flag* in the *axe1-5* mutant background (E), using
(continued)

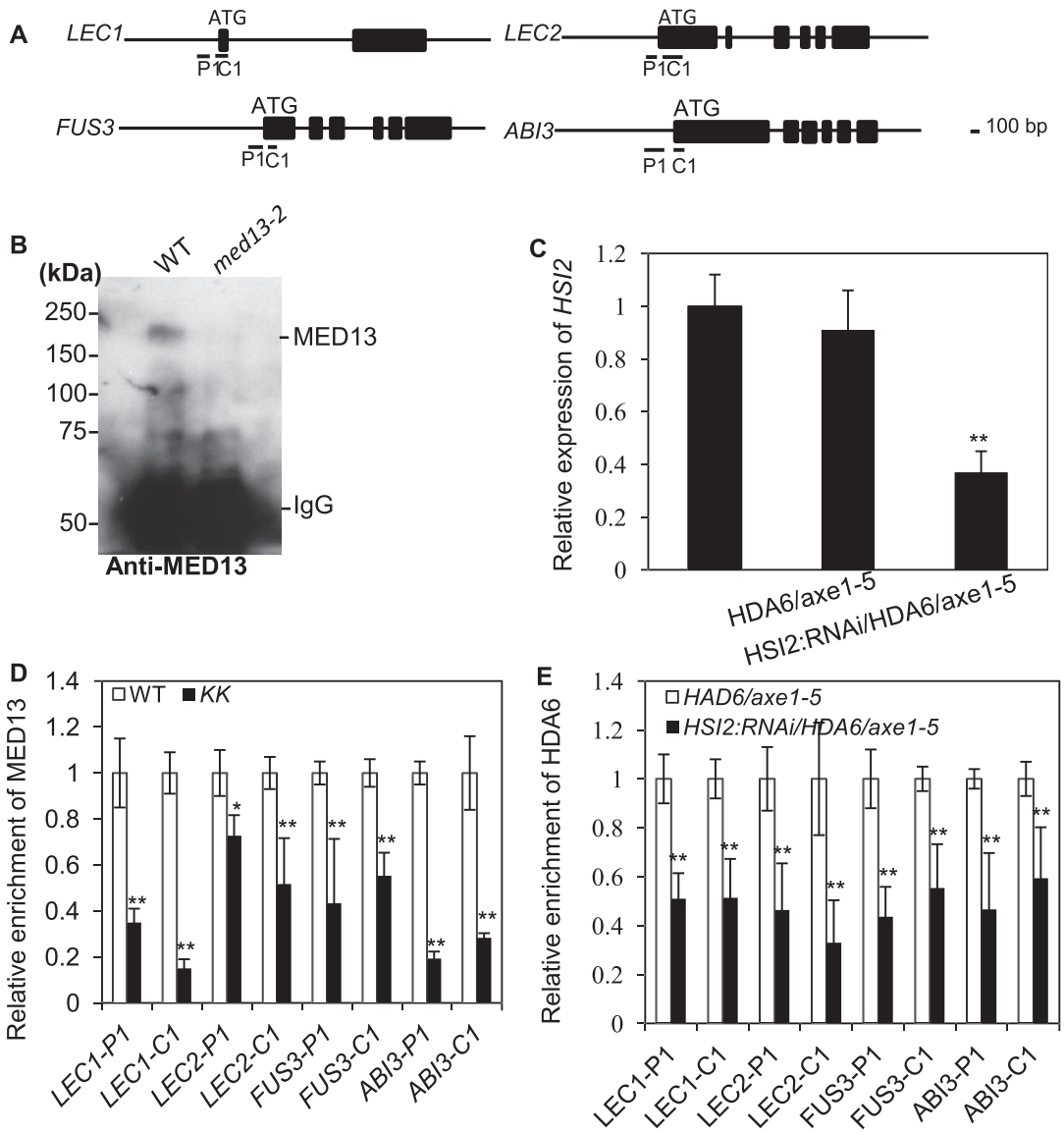


**Fig. 8** MED13 and HDA6 binding to seed maturation genes is HSI2 dependent. (A) Schematic representation of *LEC1*, *LEC2*, *FUS3* and *ABI3* loci. Genomic regions marked as P (promoter region) or C (5′-coding region near the ATG start codon) were interrogated by ChIP. The relevant genomic regions of *LEC1*, *LEC2*, *FUS3* and *ABI3* for ChIP assays are: *LEC1* (P1 = −166 to −21; C1 = +47 to +198), *LEC2* (P1 = −159 to +36; C1 = +37 to +276), *FUS3* (P1 = +5 to +157; C1 = +276 to +367) and *ABI3* (P1 = +1 to +227; C1 = +542 to 654). (B) Western blot analysis of MED13 protein by anti-MED13 of 13-day-old seedlings of the WT and *med13-2* mutant. (C) Transcription level of *HSI2* of 13-day-old seedlings of WT, *ProHDA6:HDA6-Flag/axe1-5* and *HSI2:RNAi* in *ProHDA6:HDA6-Flag/axe1-5* (*HSI2:RNAi/HDA6/axe1-5*) transgenic plants. (D and E) ChIP assays using MED13 antibody (D) or Flag antibody (E) showing relative enrichment of MED13 or HDA6 in the promoter and coding regions of *LEC1* (*LEC1-P1*; *LEC1-C1*), *LEC2* (*LEC2-P1*; *LEC2-C1*), *FUS3* (*FUS3-P1*; *FUS3-C1*) and *ABI3* (*ABI3-P1*; *ABI3-C1*) loci. Relative enrichment is shown as the qPCR value (±SE) as a percentage of input. Mean relative enrichment was normalized to a value of 1 in WT (D) or *ProHDA6:HDA6-Flag/axe1-5* (E) plants. Data are average values (±SE) of at least three biological repeats. * and ** indicate a significant difference at 5% ($P < 0.05$) and 1% ($P < 0.01$), respectively, from the WT or complemented line *HDA6/axe1-5*.

**Fig. 7** Continued

anti-GFP, HA and Flag antibody, respectively. *LEC1*, *LEC2*, *FUS3* and *ABI3* were used as key target seed maturation genes, whereas *ACT7* was used as an internal control. The region in both the promoter and coding/intron regions of seed maturation genes for ChIP assays are *LEC1* (P1 = −166 to −21; P2 = −184 to −325; P3 = −783 to −584; C1 = +47 to +198; C2 = +239 to +411; C3 = +1,203 to +1,317), *LEC2* (P1 = −159 to +36; P2 = −371 to −259; P3 = −1,047 to −932; C1 = +37 to +276; C2 = +477 to +709; C3 = +2,677 to +2,821), *FUS3* (P1 = +5 to +157; P2 = −308 to −116; P3 = −1,420 to −1,193; C1 = +267 to +367; C2 = +678 to +765; C3 = +1,790 to +1,961), *ABI3* (P1 = +1 to +227; P2 = −169 to −16; P3 = −978 to −770; C1 = +542 to +654; C2 = +732 to +930; C3 = +3,247 to +3,406), *ACT7* (P1 = −540 to −379; P2 = −1,202 to −1,009; P3 = −1,703 to −1,503; C1 = +165 to +277; C2 =+641 to +798; C3 = +1,098 to +1,254). ChIP analysis was followed by qPCR and the result was normalized for the amount of input DNA. The value of the WT was assumed to be 1. Average values ± SE ($n = 3$ biological replicates) are given. **Significantly different at the 1% level ($P < 0.01$).

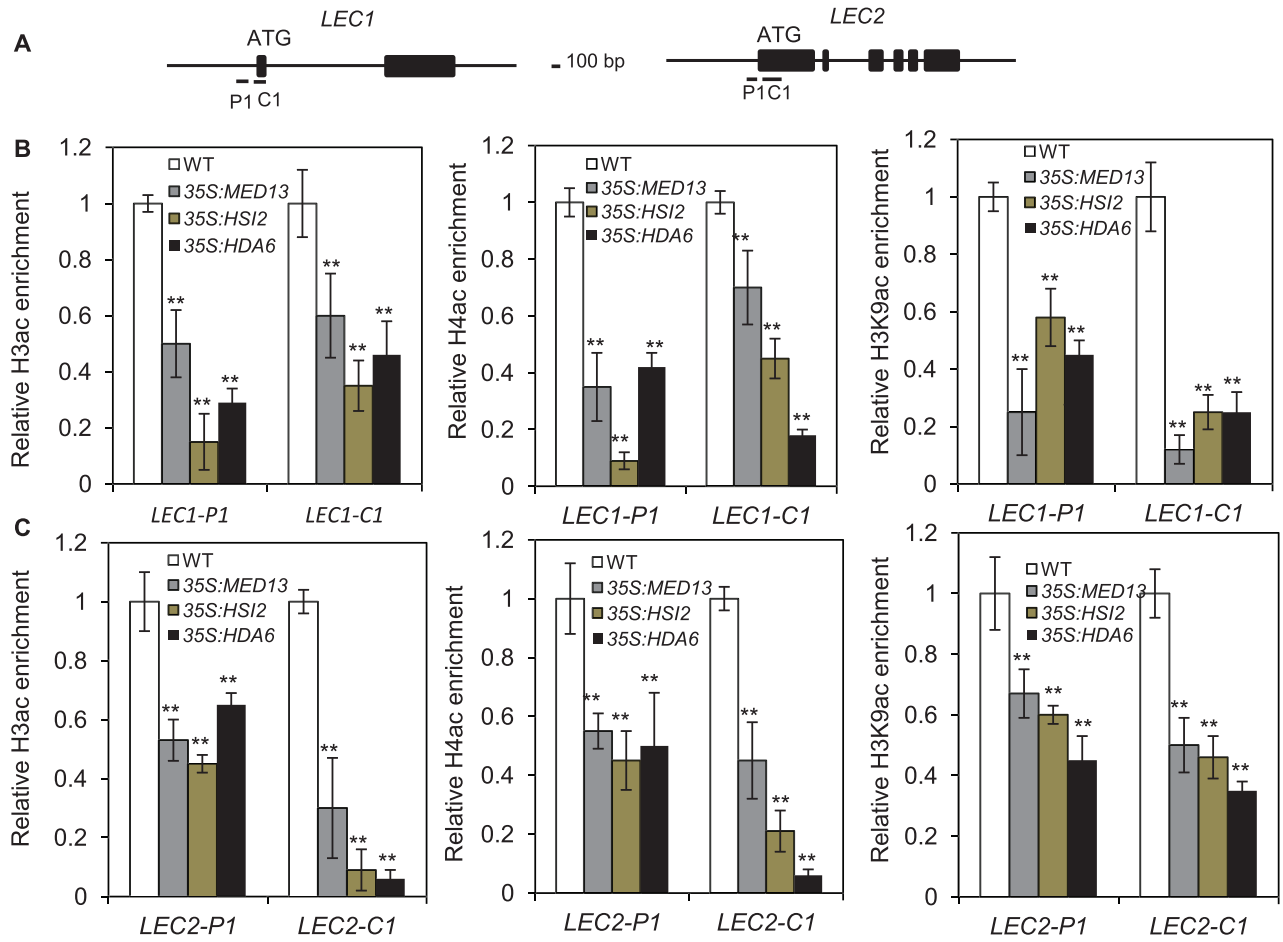


**Fig. 9** Enrichment of H3ac, H4ac and H3K9ac on the promoter and coding regions of *LEC1* (*LEC1-P1* and *LEC1-C1*) and *LEC2* (*LEC2-P1*and *LEC2-C1*) in *35S:MED13*, *35S:HSI2* and *35S:HDA6* transgenic plants. (A) Schematic representation of *LEC1* and *LEC2* loci. Genomic regions marked as P (promoter region) and C (5′-coding region near the ATG start codon) were interrogated by ChiP. The relevant genomic regions of *LEC1* and *LEC2* for ChIP assays are: *LEC1* (P1 = −166 to −21; C1 = +47 to +198) and *LEC2* (P1 = −159 to +36; C1 = +37 to +276). (B and C) Enrichment of H3ac, H4ac and H3K9ac on the promoter and coding regions of *LEC1* loci (B, upper panel) and *LEC2* loci (C, lower panel), respectively, in *35S:MED13*, *35S:HSI2* and *35S:HDA6* plants. Enrichment of H3ac, H4ac and H3K9ac is shown as the qPCR value (±SE) as a percentage of input. Mean relative enrichment in *35S:MED13*, *35S:HSI2* and *35S:HDA6* plants was normalized to a value of 1 in WT plants. Data are average values (±SE) of at least three biological repeats. **Significant difference at 1% ($P < 0.01$).

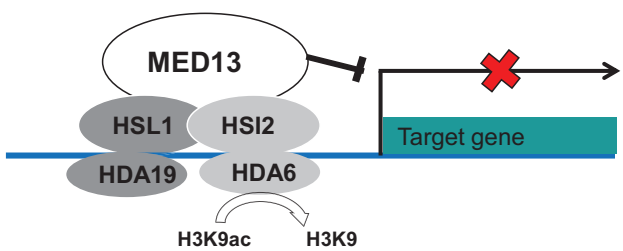


**Fig. 10** A proposed model for MED13-mediated repression of seed maturation genes. The HSI2 or HSL1 homocomplex or HSI2–HSL1 heterocomplex recognizes specific DNA sequences upstream of the promoter region of a subset of seed maturation genes (*LEC1*, *LEC2*, etc). Upon binding to the *cis*-elements, these repressors recruit the MED13 subunit of the CDK8 module thereby disrupting Pol II transcription. In addition, HSI2 recruits HDA6 and the complex enhances the effect of the HSL1–HDA19 complex (Zhou et al 2013) to erase the positive histone mark by deacetylation of H3K9/14ac.

probably followed by a sequence of biochemical events leading to the formation of repressive chromatin on these gene loci. This working model is supported by the following lines of evidence: (i) HSI2 and HSL1 form a homocomplex and heterocomplex in vivo, as shown by BiFC and Co-IP experiments; (ii) the N-terminal region of HSI2 binds to the TRAP240 domain of MED13 in vitro and in vivo; similar but less detailed results were obtained with HSL1; (iii) the C-terminal region of HSI2 binds to HDA6 whereas Zhou et al. (2013) have previously reported the interaction of HSL1 with HDA19 but not HDA6; (iv) all three proteins, HSI2, MED13 and HDA6, bind to the proximal promoter and 5′-coding regions of seed maturation genes; (v) mutant alleles of *med13* show enhanced expression of the seed maturation gene whereas the converse is true with MED13-overexpressing plants; and (vi) overexpression of MED13 cannot suppress the elevated expression of the seed maturation gene found in the *hsi2 hsl1* (*KK*) double mutant. Similar results were also found with HSI2

overexpression in the *med13* mutant compared with the WT background. These results indicate that HSI2, HDA6 and MED13 form a complex to repress seed maturation gene expression co-ordinately. The embryonic program must be repressed during seed germination in order for the embryo to complete transition to the vegetative phase of the plant life cycle (Tsukagosgi et al. 2007, Jia et al. 2014). Although HSI2 acts redundantly with HSL1 to repress seed maturation programs (Tsukagoshi et al. 2007), it is also likely that the PHD domain in the N-terminus of HSI2 alone may repress selective target genes as this domain has been reported to associate with the repressive H3K27me3 mark (Veerappan et al. 2012, Veerappan et al. 2014).

## MED13 and HDA6 bind to seed maturation genes via HSI2 dependent

Our results show that the enrichment of MED13 and HDA6 was impaired in the double mutant *KK* and *HSI2:RNAi/HDA6/axe1-5* transgenic plant, respectively, suggesting that HSI2 is required for MED13 and HDA6 to repress target genes. MED13 is a subunit of the CDK8 module which can bridge transcription factor and Pol II machinery. HDA6, on the other hand, is a histone deacetylase with no DNA binding activity. Since both MED13 and HDA6 bind to chromatin, the two proteins are probably recruited by a transcription factor/repressor to target genes. Our result supports the hypothesis that MED13 and HDA6 bind to seed maturation genes indirectly via HSI2.

## HSI2 and HSL1 interact with HDA6 and HDA19, respectively

HSI2 as well as HSL1 contain a conserved B3 DNA-binding domain located within its N-terminal half, that binds to the RY-motif found on 5′ upstream sequences of seed maturation genes (Braybrook et al. 2006, Guerriero et al. 2009). The core sequence of the RY-motif is CATGCA. We found that, like most transcription factors, these two repressors have the capacity to form homo- and heterocomplexes, suggesting that the active form may bind to target DNA sequences as such complexes. Zhou et al. (2013) reported that HSL1 but not HSI2 interacts with HDA19, whereas we show here that HSI2 but not HSL1 specifically binds to HDA6. The HDA6-interacting region on HSI2 is located on the C-terminal half of the protein (this work), and Zhou et al. (2013) have further defined the HSL1 Zf-CW domain to be required for HSL1–HDA19 association.

The functional redundancy of HSI2/HSL1 is also reflected at the level of their interacting histone deacetylases with respect to regulation of seed maturation genes. Tanaka et al. (2008) reported that *HDA6* and *HDA19* act redundantly in regulating seedling growth. Knock-down of *HDA6* expression by RNAi has no effect on seedling growth; however, additional knock-down of *HDA19* in the *HDA6:RNAi* background results in post-germination growth arrest, formation of embryo-like structures and activation of *ABI3*, *FUS3* and *LEC1*, as well as a number of seed storage protein genes. In addition to HDA6 and HDA19, class 1 of the RDP3/HDA1 superfamily of histone deacetylases also contains two other related members: HDA7 and HDA9. Recently, Van Zanten et al. (2014) reported that HDA9 negatively regulates seed germination and is required to suppress seedling traits in dry seeds probably by transcriptional repression via histone deacetylation. Possible roles of these two deacetylases in early seedling development require further investigation.

One consequence of the recruitment of HDA6/19 to seed maturation genes by the HSI2–HSL1 complex is deacetylation of positive histone marks (H3K9/14ac and H4ac) so as to help establish a repression chromatin structure. In this regard, Zhou et al. (2013) have reported an increase in H3ac, H4ac and H3K4me3 levels but a decrease in H3K27me3 levels in proximal promoter and 5′-coding regions of seed maturation genes in *hsl1* and *hda19* mutant. Here, we found that overexpression of *HSI2* or *HDA6* inhibited seed maturation gene expression and in both transgenic lines there was a decrease in H3ac and H4ac levels in the proximal promoter region and the 5′-coding region of both *LEC1* and *LEC2*. Together, these results show that HSL1/HDA19 and HSI2/HDA6 control gene expression by modulating H3ac and H4ac levels.

In addition to the B3 DNA-binding domain, HSI2/HSL1 also contain a PHD domain at the N-terminal region and a Zf-CW motif at the C-terminal region. Our results show that the Zf-CW domain but not the EAR motif mediates HSI2–HDA6 interaction. The Zf-CW motif has been recently identified to be a reader of histone marks, with specific recognition of H3K4me2 and H3K4me3 in vitro (Hoppmann et al. 2011), whereas the PHD domain may also interact with H3K4me3 (Sanchez and Zhou 2011). These results suggest that HSI2/HSL1 may mediate possible cross-talk between H3K9 deacetylation, catalyzed by HDA6 and HDA19, and H3K4me3 demethylation. These possibilities should be examined in future work. Veerappan et al. (2012) have isolated a new allele of *hsi2*, called *hsi2-4*, which suffers a missense mutation (C66Y) in the HSI2 PHD domain. Microarray analysis showed that several seed maturation genes are non-redundantly de-repressed by the *hsi2-4* mutation and these genes are also enriched in H3K27m3 marks. The recent demonstration that HSI2 also interacts with AtBMI1, a subunit of PRC1, provides a link between HSI2 and H2Aub and finally H2K27me3 (Yang et al. 2013). In addition to HSI2/HSL1, ASIL1 (Arabidopsis 6b-interacting protein 1-like 1) is also required to repress the seed maturation program by targeting GT-box-containing embryonic genes (Gao et al. 2012).

## Low frequency of *med13* mutant phenotype is partially due to low penetrance

Mutation in MED13 resulted in a variety of fused cotyledon phenotype. However, the frequency of mutants showing defective phenotypes did not follow Mendelian inheritance. About 22–33% of the plants with the mutant (*med13/med13*) genotype displayed cotyledon defects and showed severe plant growth arrest after transfer to soil, whereas the remainder (67–78%) produced normal cotyledons (**Table 1**). Consistent with this observation, only about 30% of the *MED13* RNAi plants developed distorted cotyledons whereas 70% were normal. Together, these results show that the low frequency of mutant phenotype is not caused by embryo lethality but rather is due to incomplete penetrance. Ito et al. (2011) has

reported *MED13* expression in the embryo and here we confirmed that *MED13* is active at different stages of embryogenesis. Since cotyledons are formed during later stages of embryogenesis, the cotyledon phenotype is a consequence of impaired embryogenic events. It is interesting that only 8% of the *hsi2 hsl1* (*KK*) double mutant display a tricotyledon phenotype (Tsukagoshi et al. 2007). Incomplete penetrance of the mutant phenotype has also been reported for mutations in *CUP-SHAPED COTYLEDON1* (*CUC1*), *CUC2* or *CUC3* (Hibara et al. 2006); however, double mutants and triple mutants of these genes led to almost 100% cup-shaped phenotype of cotyledon, suggesting genetic redundancy in regulating cotyledon separation (Hibara et al. 2006). In the case of *MED13*/*MAB2*/*GCT2* we could not detect any homologous gene in the Arabidopsis genome. It is quite possible that HSI2/HSL1 may also interact with other CDK8 module subunits or some as yet characterized factors.

## The TRAP240 domain of MED13 mediates repressive functions of HSI2/HSL1

We found that the repressive function of HSI2/HSL1 is mediated at least in part by their association with the TRAP240 domain of MED13. In the case of HSI2, the MED13-interacting segment is localized at the N-terminal region which also includes the B3 DNA-binding domain (**Fig. 2**). Given the sequence homology between HSI2 and HSL1, we expect a similar region of HSL1 to be involved in the binding to the MED13-TRAP240 domain as well.

Disruption of Arabidopsis *MED13* function and *MED13* overexpression led to excessive and reduced lipid accumulation in cotyledons, respectively. Gillmor et al. (2014) has recently reported accumulation of lipids in *med13*. Consistent with this observation, *MED13* is strongly expressed in cotyledons and it is expressed throughout embryogenesis. During late embryogenesis, synthesis of storage compounds ends and the embryo becomes metabolically quiescent and develops desiccation tolerance (Baud et al. 2008). Upon seed germination, *MED13* is also expressed in cotyledons concomitant with the conversion of lipid to sugar, suggesting that *MED13* acts antagonistically to lipid accumulation. Our analysis showed that *med13* mutants had high transcript levels of *LEC1*, *LEC2*, *WRI1*, *FUS3*, *Ole3*, *At2S3* and *ABI3*, whereas the opposite result was found in transgenic plants overexpressing *MED13*. Seedlings of the double mutant *hsi2 hsl1* (*KK*) showed early growth arrest and enhanced expression of seed maturation genes including *LEC1*, *ABI3* and *FUS3* (Suzuki et al. 2007, Tsukagoshi et al. 2007). Together, these results support the view that HSI2(HSL1)/MED13 form a complex to repress expression of seed maturation genes.

## Modulation of lipid accumulation by MED13 is functionally conserved among eukaryotes

The TRAP240 domain (amino acids 1,058–1,160) of Arabidopsis MED13 is well conserved among eukaryotes (**Fig. 2B**). Recent studies have implicated *MED13* as a negative regulator of lipid biosynthesis in *Drosophila* and mice (Pospisilik et al. 2010, Grueter et al. 2012). There are also other examples of functional conservation of homologous genes between animals and Arabidopsis. The *COMPARATIVE GENE IDENTIFICATION-58* (*CGI-58*) gene is a key regulator of lipid metabolism in mammals (Lass et al. 2006), and disruption of the Arabidopsis *CGI-58* homolog produced a high amount of lipid droplets in leaves (James et al. 2010). Our work here predicts the presence of transcriptional repressors in animal cells, similar to the Arabidopsis HSI2/HSL1 that would bind to MED13 and histone deacetylases to regulate lipid biosynthesis negatively.

# Materials and Methods

## Plant growth conditions

Sterilized Arabiopsis seeds were plated on medium containing full Murashige and Skoog (MS) supplemented with 1% sucrose. Plates were placed at 22°C under long-day conditions (16 h light/8 h dark cycle) under about 100 μmol $m^{-2}$ $s^{-1}$. Two week-old seedlings were transferred to soil and grown until maturity under the same light and temperature conditions.

## Plant materials

*Arabidopsis thaliana* Columbia type (Col-0) was used as the WT. The *gct2* mutant, an EMS-induced mutation, was later re-named *med13-1* Gillmor et al., 2010). Another *med13* allele used was a T-DNA insertion line (Salk_018056) named *med13-2*, obtained from the Arabidopsis Biological Resource Center (http://www.arabidopsis.org). The *axe1-5* mutant was from Dr. Keqiang Wu, National University of Taiwan, Taiwan.

## Genotyping and sequencing

Genotyping of the T-DNA insertion line (Salk_018056) was performed by PCR with three primers including left primer (LP), right primer (RP) and left border primer for T-DNA insertion (LB). The primer sequences were for LP, 5′-GTTCTT AAAACTGCCGAAGGG-3′; RP, 5′-TTGCTTTT CATTGCCTTGAAC-3′; and LB, 5′ATTTTGCCGATTTCGGAAC-3′. However, the genotyping of *gct2* (*med13-1*), an EMS-induced mutant, was performed by PCR and sequencing using two primers, forward primer 5′-ACAGAGGACTGGAGATGG-3′, and reverse primer 5′-AATCTCAGGACCTCCAGC-3′. Primers LP and RP for *hsi2-2* were 5′-GTCCA TGATGCTACAGGCTGGTGATAC-3′ and 5′-CTGCATGTCTCCAGCATTAGCT GCCT-3′, respectively. Primers LP and RP for *hsl1-1* were 5′-TCGGAACATTGGG ACTAAGAGCAAG-3′ and 5′AAGCATCACACTGCACCCATTGCT-3′, respectively.

## Microscopy and histochemical staining

*Fat Red 7B staining.* Twelve-day-old seedlings were stained overnight with 0.1% (w/v) solution of Fat Red 7B (Sigma-Aldrich) (Brudrett et al. 1991), and were then rinsed several times with distilled water before examination by light microscopy using a Leica microscope equipped with a Nikon digital camera (Dxm1200F, Japan).

*Nile Red and Bodipy493/503.* Nile Red and Bodipy493/503 staining was performed as described by Jame et al. (2010). Cotyledons detached from 12-day-old seedlings were fixed in 4% (w/v) paraformaldehyde in 50 mM PIPES (pH 7.0) and stained with 6.5 mg $ml^{-1}$ Nile Red or 5 μg $ml^{-1}$ Bodipy493/503. Lipid droplets were observed using confocal laser scanning microscopy with a Zeiss LSM 510 META microscope equipped with an Axioplan2 imaging system. Images were then processed in the Zeiss LSM Image Browser Program.

*GUS staining.* GUS activity staining was performed according to Zhang et al, (2010). Images were taken with a Leica equipped with a Nikon digital camera (Dxm1200F, Japan).

## Fatty acid extraction

Fatty acid composition and total fatty acid were analyzed according to Li et al. (2006) using detached cotyledons from 12- to 14-day-old seedlings. Samples

were analyzed using gas chromatography–mass spectrometry (GC-MS) with a Triple-Axis Detector and HP-88 column (100 m × 0.25 mm) (Agilent Technologies). The GC-MS data were analyzed using MSD ChemStation E. 02. 02. 1431 Software (Agilent Technologies).

## Plasmid constructs and plant transformation

The *ProMED13:GUS* construct was generated by cloning the native promoter region of *MED13* (−934 to −1 relative to ATG of *MED13*) into the binary vector pCAMBIA 1300-221. To generate *35S: MED13*, pDONR 221 vector (Gateway system) containing full-length MAB2/MED13 (a gift from Dr. Jun Ito, Nara Institute of Sciences and Technology, Japan) was subcloned into destination vector, pBA-DC-HA. The RNAi knockdown in the *MED13* construct was generated by amplifying and cloning sense and antisense fragments of *MED13* into pFGC5941 plasmid. cDNAs encoding HSI2 and HDA6 were amplified and cloned into binary vector pCAMBIA1300 to construct *35S:HSI2* and *35S:HDA6*. cDNA encoding HSL1 was amplified and initially cloned into pENTR/SD/D-TOPO and subcloned into pBA-DC-HA destination vector. To generate knockdown *HSI2:RNAi* in the *ProHDA6:HDA6-Flag/axe1-5* background, about 1 kb of the coding region of *HSI2* was amplified and initially cloned into pENTR/SD/D-TOPO and subcloned into RNAi destination vector pH7GWIWG2 (II). The construct containing *HSI2:RNAi* was then transformed into transgenic plants carrying *ProHDA6:HDA6-Flag/axe1-5*. Arabidopsis plants were transformed using the floral dip method (Clough and Bent, 1998, Zhang et al. 2006). The primers used for generating these constructs are listed in **Supplementary Table S2**.

## Complementation test

*ProMED13:MED13-GFP* and *Pro35S:HSI2-HA* were transformed through *Agrobacterium tumefaciens* into *med13-2* (+/−) and *hsi2 hsl1* (+/−) populations, respectively. The resulting $T_1$ generation seeds were plated and screened on MS medium containing 50 μg $ml^{-1}$ hygromycin antibiotic. Genotyping was then performed using specific primers for resistant plants.

## Quantitative real-time PCR (qRT-PCR)

Total RNA was extracted from cotyledons of 10- to 14 day-old seedlings grown with 1% sucrose, with the Dneasy Plant Mini Kit (Qiagen) following the manufacturer's instructions. RNAs from seeds, stems, roots and siliques were extracted as described by Suzuki et al. (2004). A 1 μg aliquot of total RNA was used to synthesize cDNA with th eGo Taq 2 Step RT-qPCR system (Promega) following the manufacturer's instruction, and qPCR was performed with Power SYBR® Green PCR Master Mix (Applied Biosystems by Life Technology) in a ABI 7900 RT-PCR system (Applied Biosystems). For each experiment, three replicates were performed, and *ACTIN2* (*ACT2*) was used as the reference gene. The result of qRT-PCR was determined as the expression relative to a value of 1 in WT plants. The primers used for qRT-PCR are listed in **Supplementary Table S3**.

## Protein localization

Full-length cDNA of *MED13* except the stop codon was fused to *GFP* in pCAMBIA1302 under the control of the *MED13* promoter (*ProMED13:MED13-GFP*) or 35S promoter (*Pro35S:MED13:GFP*). *Agrobacterium tumefaciens* strain AGL1 carrying the *ProMED13:MED13-GFP* or *Pro35S:MED13-GFP* construct was transformed into tobacco leaf (*N. benthamiana*). After 2–4 d infiltration, protein localization was observed by confocal laser scanning microscopy. The primers used to generate *ProMED13:MED13-GFP* and *Pro35S:MED13-GFP* constructs are listed in **Supplementary Table S2**.

## In vitro pull-down assay

The coding regions of HSI2 and HDA6 were amplified and cloned into pGEX-6p-1vector (GE Healthcare). To generate His-tagged proteins, the coding regions of MED13-NT (N-terminus of MED13), MED13-CT (C-terminus of MED13), TRAP240 (a conserved domain located between the N- and C-terminal regions of MED13), HSI2-NT (N-terminus of HSI2) and HSI2-CT (C-terminus of HSI2) were cloned into pET-28a(+) vector (Novagen). Primers used to amplify these clones are listed in **Supplementary Table S2**. GST fusion proteins were purified from *Escherichia coli* extracts using a Protino GST/4B Column (Macherey-Nagel), whereas His fusion proteins were purified using Ni–Sepharose beads (GE Healthcare). For MED13/HSI2 interaction analysis, 5 μg of GST–HSI2 or 2 μg of GST was incubated with 5 μg of His-MED13-NT, 5 μg of His-MED13-CT or 2 μg of His-TRAP240. For HSI–HDA6 interaction, 5 μg of GST–HDA6 or 2 μg of His was incubated with 5 μg of His-HSI2, 5 μg of His-HSI2-NT or 2 μg of His-HSI2-CT. Both bait and prey proteins were then mixed with immobilized GST or His beads which were rotated overnight at 4°C. Following incubation, the beads were extensively washed with binding buffer [50 mM Tris–HCl, pH 8.0, 150 mM NaCl, 5 mM EDTA, 1% Triton X-100, 1 mM dithiothreitol (DTT) in protease inhibitor cocktail tablet solution (Roche)], eluted in SDS–polyacrylamide gel loading buffers, and analyzed by SDS–PAGE. Protein–protein interaction was detected using anti-His or anti- GST antibody (Cell Science).

## BiFC analysis

For protein–protein interaction using BiFC analysis, full-length cDNA of HSI2 and HDA6, and a TRAP240 domain of MED13 were amplified and cloned into serial pSAT1 vectors containing either an N- or C-terminal enhanced yellow fluorescence protein (EYFP) fragment. The resulting construct was then subcloned into a pGreen binary vector HY105 (kindly provided by Dr. Hao Yu, National University of Singapore). For analysis of protein interaction, full-length cDNA of HSI2 and HSL1 without the stop codon was initially cloned into the pENTR/SD/D-TOPO vector and subcloned into pEarleyGate210-YN and pEarleygate202-YC vectors (Lu et al. 2010) which were provided by Dr. Keqiang Wu, National Taiwan University. *Agrobacterium tumefaciens* strain C58C1 or AGL1 carrying each clone as mentioned above was co-infiltrated into tobacco leaves. After 1–4 d infiltration, protein–protein interaction was observed using confocal laser scanning microscopy.

## Co-immunoprecipitation (Co-IP)

DNA sequences for HSI2, HSL1, the TRAP240 domain of MED13 and HDA6 were cloned into pBA-DC-HA or pBA-DC-myc. Constructs were introduced into *A. tumefaciens* strain AGL1 and infiltrated into tobacco leaves. At 2–3 d post-infiltration, total protein was extracted from tobacco leaves using lysis buffer [50 mM Tris–HCl pH.8.0, 150 mM NaCl, 10% glycerol, 1% NP-40, 2 mM EDTA, 1 mM phenylmethylsulfonylfluoride (PMSF) and protease inhibitor cocktail]. After centrifugation at 15,000 r.p.m. $min^{-1}$ for 40 min, the supernatant was incubated with protein A–agarose/salmon sperm DNA for 1–2 h for pre-clearing before incubation with 5 μg of HA antibody overnight at 4°C. A 50 μl aliquot of protein A–agarose beads was added and incubated for 1–2 h at room temperature. The beads were washed 3–4 times with washing buffer (50 mM Tris–HCl pH. 8.0, 150 mM NaCl, 0.1% NP-40, 2 mM EDTA, 1 mM PMSF and protease inhibitor cocktail). The proteins were eluted with 2.0× sample buffer and analyzed by immunoblotting using anti-myc antibody.

## Chromatin immunoprecipitation (ChIP) assay

ChIP assay was performed mainly as described (Saleh et al. 2008) with slight modification. Chromatin was extracted from cotyledons of 2-week-old seedlings grown in MS medium supplemented with 1% sucrose. The cotyledons were then treated with 1% formaldehyde and the resulting chromatin was sheared to an average length of 500 bp (200–1,000 bp) by sonication and used for immunoprecipitation with specific antibodies. Finally, DNA cross-linked to immunoprecipitated proteins was analyzed by real-time qPCR. Three biological repeats were performed in triplicate for each experiment by qPCR, and *ACT7* was used as an internal control for normalization. Primers of target genes used for real-time qPCR in ChIP analysis are listed in **Supplementary Table S4**. For binding of MED13–GFP, HSI2-HA and HDA6-FLAG to seed maturation genes, antibodies to GFP (Cell Science, CS120569B), HA (Cell sciences; CS120564B) and FLAG (Cell Sciences; CSI20568B) were used, respectively. For histone modification experiments, antibodies were purchased from Millipore: H3ac, (Millipore 06-599); H4ac (Millipore 06-866); and H3K9ac (Millipore 07-352).

## Statistical analysis

Student's *t*-test analysis was performed to compare the quantitative data between WT and mutant plants or between WT and overexpression lines.

Two groups of data for comparison in all these experiments were shown to be statistically significant at the 5% ($P < 0.05$) or 1% ($P < 0.01$) level.

## Supplementary data

**Supplementary data** are available at PCP online.

## Funding

This work was supported by National Research Foundation of Singapore [Award No: NRF-CRP7-2010-02].

## Acknowledgements

We thank Dr. Jun Ito for the full-length cDNA clone of *MAB2/MED13*, Dr. Craig Pikkard for the *ProHDA6:HDA6/axe1-5* complemented line, Dr. Kenzo Nakamura for *hsl1-1* and *hsi2-2*, Dr Akira Kikuchi for the *HDA6:RNAi* line, and Dr Keqiang Wu for *axe1-5* seeds. We also thank Dr. Hui-Wen Wu, Dr. Kian Hong Ng, Dr. Hai-Xi Sun and Subramanian Kabilan for helpful technical advice.

## Disclosures

The authors have no conflicts of interest to declare.

## References

Alonso, J.M., Stepanova, A.N., Leisse, T.J., Kim, C.J., Chen, H., Shinn, P., et al. (2003) Genome-wide insertional mutagenesis of *Arabidopsis thaliana*. *Science* 301: 653–657.

Amoutzias, G.D., Robertson, D.L., Van de Peer, Y. and Oliver, S.G. (2008). Choose your partners: dimerization in eukaryotic transcription factors. *Trends Biochem. Sci.* 33: 220–229.

Asturias, F.J., Jiang, Y.W., Myers, L.C., Gustafsson, C.M., and Kornberg, R.D. (1999) Conserved structures of mediator and RNA polymerase II holoenzyme. *Science* 283: 985–998.

Autran, D., Jonak, C., Belcram, K., Beemster, G.T., Kronenberger, J., Grandjean, O. et al. (2002) Cell numbers and leaf development in *Arabidopsis*: a functional analysis of the *STRUWWELPETER* gene. *EMBO J.* 21: 6036–6049.

Bäckström, S., Elfving, N., Nilsson, R., Wingsle, G. and Björklund, S. (2007) Purification of a plant mediator from *Arabidopsis thaliana* identifies PFT1 as the Med25 subunit. *Mol. Cell* 26: 717–729.

Baud, S., Dubreucq, B., Miquel, M., Rochat, C. and Lepiniec, L. (2008). Storage reserve accumulation in Arabidopsis: metabolic and developmental control of seed filling. *Arabidopsis Book* 6: e0113.

Beyer, K.S., Beauchamp, R.L., Lee, M-F., Gusella, J.F., Naar, A.M. and Ramesh, V. (2007) Mediator subunit MED28 (Magicin) is a repressor of muscle cell differentiation. *J. Biol. Chem.* 282: 32152–32157.

Braybrook, S.A., Stone, S.L., Park, S., Bui, A.Q., Le, B.H., Fischer, R.L., et al. (2006) Genes directly regulated by LEAFY COTYLEDON2 provide insight into the control of embryo maturation and somatic embryogenesis. *Proc. Natl. Acad. Sci. USA* 103: 3468–3473.

Brundrett, M.C., Kendrick, B. and Peterson, C.A. (1991) Efficient lipid staining in plant material with Sudan Red 7B or Fluoral Yellow 088 in polyethylene glycol-glycerol. *Biotech. Histochem.* 66: 111–116.

Canet, J.V., Dobó, A. and Tornero, P. (2012) *Non-Recognition-of-BTH4*, an Arabidopsis mediator subunit homolog, is necessary for development and response to salicylic acid. *Plant Cell* 24: 4220–4235.

Cerdán, P.D. and Chory, J. (2003) Regulation of flowering time by light quality. *Nature* 423: 881–885.

Clough, S.J. and Bent, A.F. (1998) Floral dip: a simplified method for *Agrobacterium*-mediated transformation of *Arabidopsis thaliana*. *Plant J.* 16: 735–743.

Conaway, R.C., Sato, S., Tomomori-Sato, C., Yao, T. and Conaway, J.W. (2005) The mammalian Mediator complex and its role in transcriptional regulation. *Trends Biochem. Sci.* 30: 250–255.

Davis, J.A., Takagi, Y., Kornberg, R.D. and Asturias, F.J. (2002). Structure of yeast RNA polymerase II holoenzyme: mediator confirmation and polymerase interaction. *Mol. Cell* 10: 409–415.

Ding, N., Zhou, H., Esteve, P.-O., Chin, H.G., Kim, S., Xu, X., et al. (2008) Mediator links epigenetic silencing of neuronal gene expression with X-linked mental retardation. *Mol. Cell* 31: 347–359.

Earley, K.W., Pontvianne, F., Wierzbicki, A.T., Blevins, T., Tucker, S., Costa-Nunes, P., et al. (2010) Mechanisms of HDA6-mediated rRNA gene silencing: suppression of intergenic Pol II transcription and differential effects on maintenance versus siRNA-directed cytosine methylation. *Genes Dev.* 24: 1119–1132.

Flanagan, P.M., Kelleher, R.J., Sayre, M.H., Tschochner, H. and Kornberg, R.D. (1991) A mediator required for activation of RNA polymerase II transcription in vitro. *Nature* 350: 436–438.

Finkelstein, R., Reeves, W., Ariizumi, T. and Steber, C. (2008). Molecular aspect of seed dormany. *Annu. Rev. Plant Biol.* 59: 387–415.

Gao, M.J., Lydiate, D.J., Li, X., Gjetvaj, B., Hegedus, D.D. and Rozwadowski, K. (2012) Repression of seed maturation genes by a trihelix transcriptional repressor in Arabidopsis seedling. *Plant Cell* 21: 54–71.

Gillmor, C.S., Park, M.Y., Smith, M.R., Pepitone, R., Kerstetter, R.A. and Poething, R.S. (2010) The MED12–MED13 module of mediator regulates the timing of embryo patterning in Arabidopsis. *Development* 137: 113–122.

Gillmor, C.S., Silva-Ortega, C.O., Willmann, M.R., Buendia-Monreal, M. and Poethig, R.S. (2014) The *Arabidopsis* mediator CDK8 module genes *CCT* (*MED12*) and *GCT* (*MED13*) are global regulators of developmental phase transitions. *Development* 141: 1–10.

Goldberg, R.B., De Paiva, G. and Yadegari, R. (1994) Plant embryogenesis: zygote to seed. *Science* 266: 605–614.

Grueter, C.E., van Rooij, E., Johnson, B.A., DeLeon, S.M., Sutherland, L.B., Qi, X., et al. (2012) A cardiac microRNA governs systemic energy homeostasis by regulation of MED13. *Cell* 149: 671–683.

Guerche, P., Tire, C., De Sa, F.G., De Clercq, A., Van Montagu, M. and Krebbers, E. (1990) Differential expression of the Arabidopsis 2S albumin genes and the effect of increasing gene family size. *Plant Cell* 2: 469–478.

Guerriero, G., Martin, N., Golovko, A., Sundstrom, J.F., Rask, L. and Ezcurra, I. (2009) The RY/Sph element mediates transcriptional repression of maturation genes from late maturation to early seedling growth. *New Phytol.* 184: 552–565.

Hibara, K., Karim, M.R., Takada, S., Taoka, K., Furutani, M., Aida, M. and Tasaka, M. (2006) *Arabidopsis CUP-SHAPED COTYLEDON3* regulates postembryonic shoot meristem and organ boundary formation. *Plant Cell* 18: 2946–2957.

Holdsworth, M.J., Bentsink, L. and Soppe, W.J. (2008) Molecular networks regulating Arabidopsis seed maturation, after-ripening, dormancy and germination. *New Phytol.* 179: 33–54.

Hoppmann, V., Thorstensen, T., Kristiansen, P.E., Veiseth, S.V., Rahman, M.A., Finne, K., et al. (2011) The CW domain, a new histone recognition module in chromatin proteins. *EMBO J.* 30: 1939–1952.

Ito, J., Sono, T., Tasaka, M. and Furutani, M. (2011) *MACCHI-BOU 2* is required for early embryo patterning and cotyledon organogenesis in *Arabidopsis*. *Plant Cell Physiol.* 52: 539–552.

James, C.N., Horn, P.J., Case, C.R., Gidda, S.K., Zhang, D., Mullen, R.T., et al. (2010) Disruption of the *Arabidopsis* CGI-58 homologue produces chanarin-dorfman-like lipid droplet accumulation in plants. *Proc. Natl. Acad. Sci. USA* 107: 17833–17838.

Jia, H., Suzuki, M. and McCarty, D.R. (2014) Regulation of the seed to seedling developmental phase transition by the LAFL and VAL transcription factor networds. *Wiley Interdiscip. Rev. Dev. Biol.* 3: 135–145.

Koleske, A.J., and Young, R.A. (1994) An RNA polymerase II holoenzyme responsive to activators. *Nature* 368: 466–469.

Kornberg, R.D. (2005) Mediator and the mechanism of transcriptional activation. *Trends Biochem. Sci.* 30: 235–239.

Kroj, T., Savino, G., Valon, C., Giraudat, J. and Parcy, F. (2003) Regulation of storage protein gene expression in Arabidopsis. *Development* 130: 6065–6073.

Lass, A., Zimmermann, R., Haemmerle, G., Riederer, M., Schoiswohl, G., Schweiger, M., et al. (2006) Adipose triglyceride lipase-mediated lipolysis of cellular fat stores is activated by CGI-58 and defective in Chanarin–Dorfman syndrome. *Cell Metab.* 3: 309–319.

Li, Y., Beisson, F., Pollard, M. and Ohlrogge, J. (2006) Oil content of *Arabidopsis* seeds: the influence of seed anatomy, light and plant-to-plant variation. *Phytochemistry* 67: 904–915.

Lotan, T., Ohto, M., Yee, K.M., West, M.A.L., Lo, R., Kwong, R.W., et al. (1998) *Arabidopsis* LEAFY CONTYLEDON1 is sufficient to induce embryo development in vegetative cells. *Cell* 93: 1195–1205.

Lu, Q., Tang, X., Tian, G., Wang, F., Liu, K., Nguyen, V., et al. (2010). Arabidopsis homolog of the yeast TREX-2 mRNA export complex: components and anchoring nucleoporin. *Plant J.* 61: 259–270.

Luerben, H., Kirik, V., Herrmann, P. and Misera, S. (1998) FUSCA3 encodes a protein with a conserved VP1/ABI3-like B3 domain which is of functional importance for the regulation of seed maturation in Arabidopsis thaliana. *Plant J.* 15: 755–764.

Maeo, K., Tokuda, T., Ayame, A., Mitsui, N., Kawai, T., Tsukagoshi, H., et al. (2009) An AP2-type transcription factor, WRINKLED1, of Arabidopsis thaliana binds to the AW-box sequence conserved among proximal upstream regions of genes involved in fatty acid synthesis. *Plant J.* 60: 476–487.

Malik, S. and Roeder, R.G. (2005) Dynamic regulation of pol II transcription by the mammalian Mediator complex. *Trends Biochem. Sci.* 30: 256–263.

Murfett, J., Wang, X.J., Hagen, G. and Guilfoyle, T.J. (2001) Identification of Arabidopsis histone deacetylase HDA6 mutants that affect transgene expression. *Plant Cell* 13: 1047–1061.

Nambara, E., Naito S. and McCourt, P. (1992) A mutant of Arabidopsis which is defective in seed development and storage protein accumulation is a new *abi3* allele. *Plant J.* 2: 435–441.

Ng, D.W., Chandrasekharan, M.B. and Hall, T.C. (2006) Ordered histone modifications are associated with transcriptional poising and activation of the *pheseolin* promoter. *Plant Cell* 18: 119–131.

Ohlrogge, J. and Browse, J. (1995) Lipid biosynthesis. *Plant Cell* 7: 957–970.

Pospisilik, J.A., Schramek, D., Schnidar, H., Cronin, S.J.F., Nehme, N.T., Zhang, X., et al. (2010) *Drosophila* genome-wide obesity screen reveals hedgehog as a determinant of brown versus white adipose cell fate. *Cell* 140: 148–160.

Poss, Z.C., Ebmeier, C.C. and Taatjes, D.J. (2013) The mediator complex and transcription regulation. *Crit. Rev. Biochem. Mol. Biol.* 48: 575–608.

Saleh, A., Alverez-Venegas, R. and Avramova, Z. (2008) An efficient chromatin immunoprecipitation (ChIP) protocol for studying histone modifications in *Arabidopsis* plants. *Nat. Protoc.* 3: 1018–1025.

Sanchez, R. and Zhou, M.M. (2011) The PHD finger: a versatile epigenome reader. *Trends Biochem. Sci.* 36: 364–372.

Siloto, R.M., Findlay, K., Lopez-Villalobos, A., Yeung, E.C., Nykiforuk, C.L. and Moloney, M.M. (2006) The accumulation of oleosins determines the size of seed oilbodies in Arabidopsis. *Plant Cell* 18: 1961–1974.

Stone, S.L., Kwong, L.W., Yee, K.M., Pelletier, J., Lepiniec, L., Fischer, R.L., et al. (2001) *LEAFY COTYLEDON2* encodes a B3 domain transcription factor that induces embryo development. *Proc. Natl. Acad. Sci. USA* 98: 11806–11811.

Suzuki, M. and McCarty, D.R. (2008) Functional symmetry of the B3 network controlling seed development. *Curr. Opin. Plant Biol.* 11: 548–553.

Suzuki, M., Wang, H.H. and McCarty, D.R. (2007) Repression of the LEAFY COTYLEDON 1/B3 regulatory network in plant embryo development by VP1/ABSCISIC ACID INSENSITIVE 3-LIKE B3 gene. *Plant Physiol.* 143: 902–911.

Suzuki, Y., Kawazu, T. and Koyama, H. (2004) RNA isolation from siliques, dry seeds, and other tissues of Arabidopsis thaliana. *BioTechniques*, 37: 542–544.

Tanaka, M., Kikuchi, A. and Kamada, H. (2008) The Arabidopsis histone decetylases HDA6 and HDA19 contribute to the repression of embryonic properties after germination. *Plant Physiol.* 146: 149–161.

Theodoulou, F.L. and Eastmond, P.J. (2012) Seed storage oil catabolism: a story of give and take. *Curr. Opin. Plant Biol.* 15: 322–328.

Tsukagoshi, H., Morikami, A. and Nakamura, K. (2007) Two B3 domain transcriptional repressors prevent sugar-inducible expression of seed maturation genes in *Arabidopsis* seedlings. *Proc. Natl. Acad. Sci. USA* 104: 2543–2547.

Tsukagoshi, H., Saijo, T., Shibata, D., Morikami, A. and Nakamura, K. (2005) Analysis of a sugar response mutant of *Arabidopsis* identified a novel B3 domain protein that functions as an active transcriptional repressor. *Plant Physiol.* 138: 675–685.

Tsutsui, T., Fukasawa, R., Shinmyouzu, K., Nakagawa, R., Tobe, K., Tanaka, A., et al. (2013) Mediator complex recruits epigenetic regulatiors via its two cyclin-dependent kinase subunits to repress transcription of immune response genes. *J. Biol. Chem.* 288: 20955–20965.

Van Zanten, M., Zoll, C., Wang, Z., Philipp, C., Carles, A., Li, Y., et al. (2014) Histone deacetylase 9 represses seedling traits in *Arabidopsis thaliana* dry seeds. *Plant J.* 80: 475–488.

Veerappan, V., Chen, N., Reichert, A.I. and Allen, R.D. (2014) HSI2/VAL1 PHD-like domain promotes H3K27 trimethylation to repress the expression of seed maturation genes and complex transgenes in Arabidopsis seedlings. *BMC Plant Biol.* 14: 293–3010.

Veerappan, V., Wang, J., Kang, M., Lee, J., Tang, Y., Jha, AK., et al. (2012) A novel HSI2 mutation in Arabidopsis affects the PHD-like domain and leads to derepression of seed-specific gene expression. *Planta* 236: 1–17.

West, M.A. and Harada, J.J. (1993) Embryogenesis in higher plant: an overview. *Plant Cell* 5: 1361–1369.

Zhang H., Han, W., De Smet, I., Talboys, P., Loya, R., Hassan, A., et al. (2010) ABA promotes QC quiescence and suppresses stem cell differentiation in the *Arabidopsis* primary root meristem. *Plant J.* 64: 764–774.

Zhang, X., Henriques, R., Lin, S.-S., Niu, Q.-W. and Chua, N.-H. (2006) *Agrobacterium*-mediated transformation of *Arabidopsis thaliana* using the floral dip method. *Nat. Protoc.* 1: 641–646.

Zhou, Y., Tan, B., Luo, M., Li, Y., Liu, C., Chen, C., et al. (2013) Histone deacetylase19 interacts with HSL1 and participates in the repression of seed maturation genes in Arabidopsis seedlings. *Plant Cell* 25: 134–148.

Yang, C., Bratzel, F., Hohmann, N., Koch, M., Turck, F. and Calonje, M. (2013) VAL- and AtBMI1-mediated H2Aub initiate the switch from embryonic to postgerminative growth in Arabidopsis. *Curr. Biol.* 23: 1324–1329.